

**NON-SELECTIVE AREA DOPING OF
RARE-EARTH MATERIAL
WITH CO-DOPING**

YAP YEN

**SUBMISSION OF DISSERTATION FOR
THE FULFILLMENT OF THE
MASTER OF TECHNOLOGY
(MATERIALS SCIENCE)**

2009

UNIVERSITI MALAYA
ORIGINAL LITERARY WORK DECLARATION

Name of Candidate: Yap Yen (I.C/Passport No: 840531-05-5142)

Registration/Matric No: SGG070004

Name of Degree: Master of Technology (Materials Science)

Title of Project Paper/Research Report/Dissertation/Thesis (“this Work”):

Non-Selective Area Doping of Rare-Earth Material with Co-doping

Field of Study: Photonic

I do solemnly and sincerely declare that:

- (1) I am the sole author/writer of this Work;
- (2) This Work is original;
- (3) Any use of any work in which copyright exists was done by way of fair dealing and for permitted purposes and any excerpt or extract from, or reference to or reproduction of any copyright work has been disclosed expressly and sufficiently and the title of the Work and its authorship have been acknowledged in this Work;
- (4) I do not have any actual knowledge nor do I ought reasonably to know that the making of this work constitutes an infringement of any copyright work;
- (5) I hereby assign all and every rights in the copyright to this Work to the University of Malaya (“UM”), who henceforth shall be owner of the copyright in this Work and that any reproduction or use in any form or by any means whatsoever is prohibited without the written consent of UM having been first had and obtained;
- (6) I am fully aware that if in the course of making this Work I have infringed any copyright whether intentionally or otherwise, I may be subject to legal action or any other action as may be determined by UM.

Candidate’s Signature

Date 3rd November 2009

Subscribed and solemnly declared before,

Witness’s Signature

Date 3rd November 2009

Name: Harith Ahmad

Designation: Lecturer

ABSTRACT

In this dissertation, erbium/aluminium (Er/Al) and erbium/ytterbium (Er/Yb) codoped on silica-on-silicon waveguide films were fabricated by flame hydrolysis deposition (FHD) via solution doping. Based on the morphology and microstructure observations, the layers pre-sintered around 800°C provide the best surface adherence for solution doping. A few process parameters involved in solution doping has been investigated to study the impregnation of rare-earth in planar waveguide. It is observed that the solution strength and dipping period strongly influenced the RE concentration in silica film. Multiple solution doping method was demonstrated in the present work. The results indicated that the multiple cycles of solution doping of the soot layer increases the rare-earth concentration in the glass layer.

ABSTRAK

Dalam disertasi ini, pendopan unsur-unsur erbium/aluminium (Er/Al) dan erbium/ytterbium (Er/Yb) pada pandu gelombang jenis silika-atas-silikon telah difabrikasikan dengan gabungan kaedah mendapan secara hidrolisis api dan pendopan menggunakan pelarut. Berdasarkan pemerhatian morfologi dan mikrostruktur, lapisan sampel yang telah disinterkan separa pada sekitar 800°C mempunyai ciri pelekapan permukaan yang paling memuaskan untuk proses pendopan menggunakan pelarut. Penyelidikan ke atas beberapa pengubah parameter bagi kaedah pendopan menggunakan pelarut telah dilaksanakan untuk mengetahui tentang pendopan unsur bumi-nadir dalam pandu gelombang jenis planar. Didapati bahawa parameter seperti kepekatan pelarut dan masa pencelupan telah mempengaruhi kandungan unsur bumi-nadir dalam lapisan silika. Di samping itu, kaedah pengulangan proses pendopan menggunakan pelarut telah ditunjukkan dalam kajian ini. Berdasarkan keputusan yang diperolehi, kaedah pengulangan pendopan ini berjaya menambahkan kandungan bumi-nadir dalam lapisan kaca.

Acknowledgements

This is a great opportunity to express my respect to my supervisor – Prof. Harith Ahmad - for his support and advice. This dissertation could not have been written without Dr. Faisal Rafiq who not only served as my co-supervisor but also encouraged and guided me through the dissertation process.

I wish to thank my colleagues who have always willing to offer their helps. They have provided me with necessary assistance and useful advice: Pua Chang Hong, Lim Weng Hong, Kow Siew Ting, Chong Wu Yi, Alvin Law, Sua Yong Meng and Tan Chin Chong.

Special thanks to Mr. Shahril for his cooperation in providing machine for my samples characterization.

Finally, my greatest gratitude goes to my parents, Yap Yook Cheang and How Kim Hong, for being so supportive and inspiring.

List of Publication

- 1) Kow, S. T., Y. Yap, C. H. Pua, W. Y. Chong, A. W. P. Law, F. R. Mahamd Adikan, A. S. M. A. Haseeb & H. Ahmad, “Selective area rare-earth doping of planar glass samples for monolithic integration of optical passive and active waveguides.” *Optik*. Article In Press.

Contents

	Page
Front Page	i
Declaration	ii
Abstract	iii
Abstrak	iv
Acknowledgements	v
List of Publication	vi
Contents	vii
List of Figures	x
List of Tables	xii
Chemical Names	xii
Abbreviations	xiii
1 Introduction	1
1.1 Optical Network	1
1.2 Optical Amplifiers	2
1.3 Rare-earth Doped Waveguide Amplifiers	4
1.4 Existing EDWAs Fabrication Technologies	7
1.5 Proposal of the Study	7
1.6 Thesis Outline	8
References	10

2 Introduction to Glass	18
2.1 Glass Structure	19
2.1.1 Germanosilicate Glass	24
2.1.2 Phosphosilicate Glass	25
2.1.3 Borosilicate Glass	28
2.2 Active Element Doped Glass	30
2.2.1 Low Solubility	31
2.2.2 Clustering	32
2.2.3 Host Material	34
2.3 Optical Amplification	35
2.3.1 Theory of optical amplification	35
2.3.2 Amplification in 2-level and 3-level Systems	36
2.3.3 Theory of Erbium Amplification	38
2.3.4 Theory of Co-Doped Amplification	41
References	43
3 Principles and Methods of Fabrication	51
3.1 Planar Glass Samples	52
3.1.1 Flame Hydrolysis Deposition (FHD)	52
3.1.2 Sintering	57
3.2 Solution Doping	59
3.2.1 Principles of Solution Doping	59
3.2.2 Solvent	59
3.2.2.1 Water	60
3.2.2.2 Alcohol	61

3.2.3 Solute	62
3.2.4 Methodology	63
References	66
4 Results and Discussions	73
4.1 Pre-sinter Temperature	73
4.2 Fully-sintered and Half-sintered Doped Silica Films	75
4.3 Effect of Erbium Concentration	78
4.4 Effects of Aluminium in Erbium Doped Silica Films	79
4.5 Effects of Ytterbium in Erbium Doped Silica Films	81
4.6 Aluminium and Ytterbium in Co-doping	85
4.7 Immersion Period	87
4.8 Multiple Solution Doping	89
References	92
5 Conclusion and Future Work	94
5.1 Conclusion	94
5.2 Future Work	97

List of Figures

Chapter 2 Introduction to Glass		Page
2.1	Chemical structure of silica matrix.	19
2.2	Periodic table.	21
2.3	(a) Schematic of three-dimensional tetrahedral arrangement in fused silica glass; (b) Two-dimensional arrangement of silicon and oxygen atoms in cristobalite.	22
2.4	Schematic of a disrupted silica glass structure by addition of modifier ions.	23
2.5	Inclusion of Ge atom within silica matrix.	24
2.6	Schematic of three-dimensional tetrahedral arrangement for phosphate glass; showing double bond between one oxygen and the phosphorus.	25
2.7	Inclusion of P atom within a silica matrix.	26
2.8	Phase diagram representing Phosphorus doping of silica.	27
2.9	Effect of dopants upon refractive index at 598 nm.	28
2.10	Two-dimensional arrangement of boron and oxygen atoms in borate glass.	28
2.11	Inclusion of B atom within silica matrix.	29
2.12	Two-level amplification system. (a) RE at rest, (b) lower case pumping by external optical energy, (c) emission by stimulation.	36
2.13	Three-level amplification system. (a) RE at rest, (b) pumping by 980nm light source, (c) non-radiative relaxation to metastable level, (d) stimulated emission.	37-38
2.14	The up-conversion process illustrated for Er^{3+} . (a) both interacting ions are excited to the metastable $^4I_{13/2}$ level, (b) the donor ion transfers all its energy to the acceptor, leaving itself in the ground state and the acceptor in the $^4I_{13/2}$ state. For oxide glasses, the acceptor ion quickly decays nonradiatively back to the $^4I_{13/2}$ level.	40
2.15	15 Energy transfer process for the $\text{Yb}^{3+}/\text{Er}^{3+}$ co-doped system. (a) excitation of Yb^{3+} ion, (b) standard radiative decay of Yb^{3+} , (c) energy transfer ($\text{Yb}^{3+} \rightarrow \text{Er}^{3+}$), (d) energy back transfers ($\text{Er}^{3+} \rightarrow \text{Yb}^{3+}$), (e) Er^{3+} decay nonradiatively to metastable state, (f) emission by stimulation.	42
Chapter 3 Fabrication Principles and Methods		
3.1	Fabrication stages of RE-doped silica-based waveguide.	53
3.2	Gas supply system for FHD.	54
3.3	Schematic of typical Flame Hydrolysis Deposition process.	55
3.4	Diagram showing the temperature and time parameters for full-sintering of underclad/core.	58
3.5	Diagram showing temperature and time control for half-sintering of soot layer.	59
3.6	Schematic showing the solution doping process of a quarter wafer.	64

Chapter 4 Results and Discussions

4.1	SEM images of porous pre-sintered FHD layers at various pre-sintering temperatures; (a) 500°C, (b) 750°C, and (c) 800°C.	73
4.2	Defects induced by solution doping (a) 500°C (b) 750°C (c) 800°C.	74
4.3	Variation of Al and Er concentration in planar film with change in Al solution concentration for a fixed 0.02M Er solution.	75
4.4	Variation of Al and Er concentration in planar film with change in Al solution concentration for a fixed 0.04M Er solution.	76
4.5	Variation of Al and Er concentration in planar film with change in Er solution concentration for a fixed 0.4M Al solution.	76
4.6	The variation of Er concentration in the silica films as a function of Er solution concentration.	78
4.7	The variation of Al concentration in silica film as a function of Al solution concentration.	79
4.8	The variation of Er concentration in silica film as a function of Al solution concentration.	79
4.9	Variation of Er and Yb ions concentration in silica film as a function of Yb solution concentration (Er solution concentration fixed at 0.02M).	81
4.10	Refractive index of Er/Yb doped silica films as a function of Yb solution concentration.	82
4.11	Variation of Er and Yb ions concentration in silica film as a function of Er solution concentration (Yb solution concentration fixed at 0.02M).	83
4.12	Refractive index of Er/Yb doped silica films as a function of Er solution concentration.	84
4.13	The variation of Al and Yb dopants concentration as a function of Al and Yb co-dopants solution concentration.	85
4.14	The variation of Er concentration in silica film as a function of Al and Yb co-dopants solution concentration.	85
4.15	The variation of Er and Yb ions concentration as a function of immersion period.	87
4.16	Variation of refractive index of Er/Yb doped silica films as a function of immersion period.	88
4.17	Er and Yb ions incorporation in silica film as a function of the number of doping cycles.	89
4.18	Silica wafer indicating opalescence due to multiple solution doping (a) two doping cycles (b) three doping cycles.	90
4.19	Variation of refractive index of Er/Yb doped silica films as a function	91

List of Tables

Chapter 1 Introduction

- | | | |
|-----|---|---|
| 1.1 | Comparison of various optical amplifier technologies around 1550 nm operating wavelength. | 3 |
| 1.2 | Fabrication methods for EDWAs. | 7 |

Chapter 3 Fabrication Principles and Methods

- | | | |
|-----|----------------------------------|----|
| 3.1 | Recipe “Core 26”. | 55 |
| 3.2 | Solution strength for co-doping. | 64 |

Chemical Names

SiO ₂	Silicon dioxide (silica)
GeO ₂	Germanium dioxide
P ₂ O ₅	Phosphorus pentoxide
PO ₄	Phosphate
B ₂ O ₃	Boric oxide
SiCl ₄	Silicon tetrachloride
GeCl ₄	Germanium tetrachloride
POCl ₃	Phosphorus oxytrichloride
BCl ₃	Boron trichloride
Al ₂ O ₃	Aluminium oxide
Nd ₂ O ₃	Neodymium oxide
HCl	Hydrochloric acid
AlCl ₃ .6H ₂ O	Aluminium trichloride hexahydrate
ErCl ₃ .6H ₂ O	Erbium trichloride hexahydrate
YbCl ₃ .6H ₂ O	Ytterbium trichloride hexahydrate
CaO	Calcium oxide
MgO	Magnesium oxide

Abbreviations

DWDM	Densed Wavelength Division Multiplexer
ROADMs	Reconfigurable Optical Add Drop Multiplexers
FTTH	Fiber-To-The-Home
SOA	Semiconductor Amplifiers
EDFA	Erbium Doped Fiber Amplifier
RE-DWA	Rare-Earth Doped Waveguide Amplifier
EDWA	Erbium Doped Waveguide Amplifier
PLC	Planar Lightwave Circuit
PECVD	Plasma Enhanced Chemical Vapour Deposition
FHD	Flame Hydrolysis Deposition
RE	Rare Earth
EDS	Energy Dispersive Spectrometry
SEM	Scanning Electron Microscopy
CRN	Continuos-Random-Network
UV	Ultra-Violet
RIE	Reactive Ion Etching
MFC	Mass Flow Controller
MCVD	Modified Chemical Vapour Deposition
VAD	Vapour Axial Deposition

CHAPTER 1

INTRODUCTION

1.1 OPTICAL NETWORK

The first generation of optical networks emerged as early as the 1960s. Work in installing the first point-to-point connection was completed in the 1980s. This point-to-point connection utilized 800nm signals [1-3]. As such, the signal can only be transmitted about 15km distance without amplification. The deployment of additional fiber for capacity expansion is considerably expensive as there are no branching, routing or multiplexer components available. Around 1982, a large-scale optical network has been deployed due to the deregulation in the telecommunications industry, which in turn resulting the long-haul telecommunications being carried out using optical fiber systems [4].

In the 1990s, the advent of Densed Wavelength Division Multiplexer (DWDM) has led to the rapid expansion of network capacity at lower cost. This is due to the availability of low cost broadband optical amplifiers and dense wavelength filtering technique, where transmission was performed by multiplexing few frequencies in a single optical fiber. The DWDM transmission systems consist of operating wavelength utilized at 1550nm and a capacity increment range from 45Mb/s to 1.7Gb/s. Current optical networks are strongly dependent on Reconfigurable Optical Add Drop Multiplexers (ROADMs), which is also based on PLC integration technology. ROADMs allow for high-speed data services, grid computing and “triple play” [3]. The operating wavelength has switched to 1550nm.

The primary drive for the change in the network is due to the continually increasing demand for the enormous communication system capacity in the network. This is the impact shown by tremendous growth of users surfing the Internet and the World Wide Web [5]. The conventional copper cabling systems have evolved over the years in order to overcome the bandwidth limitation, however, the effective length of copper cable is eventually limited as the data rates increase [6].

Optical fiber provides high bandwidth [7], excellent signal integrity, noise immunity and applicable in long-haul transmission. Besides, optical fiber is less susceptible to certain kind of electromagnetic interferences [5]; hence it is somehow electrically isolated. All of the above shows that optical fiber has the capability far beyond the limitation of copper and therefore is an alternative solution to the copper system limitation. Optical networks not only promise to provide enormous capacity in the network but with the technological advances and the good innovation in fiber installation techniques, optical network construction is also much more economical [5-6]. Hence, many have moved slowly on fiber to the home (FTTH) deployments over cost concerns.

1.2 OPTICAL AMPLIFIERS

Optical network limitation during optical signal transmission is denoted as either dispersion limited or loss limited. In the mid-1980s, dispersion-shifted fibers have been implemented to overcome the dispersion limitation [8]. Meanwhile, loss limitation cause by attenuation (signal weakening) was overcome using optical amplifier [5].

Generally, optical amplifier is the optical fiber device that used to reduce the required pump power in order to observe a gain in glass medium. The optical laser were first suggested in the 1960s by Snitzer and co-workers [9-10] and revisited by Stone and Burrus [11] in the 1970s using the nonlinear effect of transmission fiber as gain medium [12], semiconductor amplifiers [13], rare-earth doped optical waveguides [10] and erbium-doped-fiber amplifiers [14]. The properties of the various optical amplifiers are compared base on 1550 nm wavelength band in Table 1.1.

Table 1.1 Comparison of various optical amplifier technologies around 1550 nm operating wavelength (table from [8]).

Property	Raman Amplifier	Brillouin Amplifier	SOA	EDFA	RE-DWA
Small-signal gain	>40 dB	>40 dB	>30 dB	>50 dB	20 dB
Efficiency	0.08 dB/mW	5.5 dB/mW	28 dB/mA	11 dB/mA	0.1 dB/mW
Output power	1 W	1 mW	>0.1 W	>0.5 W	2 mW
Distortion/ Crosstalk	Negligible	Negligible	Significant	Negligible	Negligible
Dynamic performance	>20 Gb/s	<100 MHz	>25 Gb/s	>100 Gb/s	>100 Gb/s
Gain bandwidth	A few tens of nm	<100 MHz	60-70 nm	30 nm	A few tens of nm
Noise figure	3 dB	>15 dB	5-7 dB	3 dB	>3 dB
Polarization sensitivity	Significant	None	<A few dB	Insignificant (<0.1 dB)	<1 dB
Coupling loss (to fiber)	<1 dB	<1 dB	A few dB	<1 dB	

Rare-earth doped optical fiber not only provides excellent influences in the field of optical communication [15] but its long lengths interaction which allows low doping level of rare earth ions leads to good doping uniformity and heat dissipation [16]. Erbium doped fiber amplifier (EDFA) has been the most concerned device as it is capable in amplifying input signals with different bit rates or formats, and can be used to amplify multiple wavelengths [5] optical signals with a wide spectral region [8].

Besides, EDFAs offer a list of outstanding properties and it includes high gain, low threshold powers, large gain bandwidths ($\approx 30\text{nm}$) [16], efficient in high-power conversion, low noise and crosstalk, high saturation power, not sensitive in polarization [5], contain broad spectral bandwidth, essentially low-coupling losses, and low cost.

Even so, there is a strong incentive on reducing the size and cost of EDFAs by miniaturization and improved packaging for applications in metro network. In this case, erbium-doped waveguide amplifiers (EDWAs) are the suitable choice as it can be constructed in arrays and combined with pump lasers and filters [17]. Analogous to the EDFA, EDWA is also used as a medium to boost up an optical signal. EDWA is a Planar Lightwave Circuit (PLC) type optical amplifier. Due to its compact physical size, integrability into monolithic multi-functional optical devices and easy mass-production, many have switched the attention to the planar type device.

1.3 RARE-EARTH DOPED WAVEGUIDE AMPLIFIERS

A great deal of research has been focused on the development of planar waveguide since the laser action from a rare-earth thin film was first demonstrated in the early seventies [18]. Although planar waveguide device have not reach similar maturity as the fiber, it is potentially more versatile than optical fiber. Planar geometry sustains the benefits from the guided-wave resonator with a more compact monolithic format which is compatible with the concepts and techniques of an integrated optics [19-21]. Furthermore, planar waveguides are not just perform as the low-power integrated optics, but such slab geometry is capable to improve the thermal limitations over cylindrical geometries [22-23].

The obvious aspect that differentiates rare-earth-doped waveguide from fiber amplifiers is that the rare-earth material is imbedded in a planar optical waveguide instead of a fiber [8]. Miniaturization of rare-earth-doped waveguide in monolithic integration form is attractive as it provides long term stability, immunity to the environmental influences of pressure and thermal, possibility in hybrid integration to form a multi-function module, and eliminate the issues of alignment inherent in fiber or bulk based optics [24]. Monolithic integration which simply means integration of multifunctional circuits on the same chip has been the ultimate solution for integration of silica waveguide devices. However, this monolithic approach is immature and still at the research stage; several issues has to be overcome such as production cost, chip yield rate, packaging matter (eg. thermal management, stress management, and electrical wiring stability) base on the current technology status [25].

The EDWAs planar design brought up two significant factors to be considered. Firstly, rare-earth-doped waveguide's dimension itself attributes to a larger background loss which is in several orders of magnitude (~ 0.1 dB/cm) greater than in fiber [8]. Shorter path lengths and higher propagation loss make it necessary to impregnated higher rare-earth-dopant concentration [8, 16] in a relatively short planar waveguides for a reasonable amplification gain [26]. Due to the high rare-earth concentration, the interaction between ion increased [16] causing the issues of energy transfer among rare-earth ions occurred and this will lead to degradation in amplifier efficiency [27] by scattering loss, non-radiative emission, etc [26].

Nevertheless, EDWAs with a maximum gain of 13.5 dB and 20 dB has been successfully demonstrated. Besides erbium, other rare-earths (eg. Nd, Yb, Pr) are also used to form waveguide amplifier. More work has been attended on the EDWA due to its emission wavelength at 1550 nm which is compatible to the operating wavelength used in the fiber technology. Based on the result, RE-DWAs are seen to have huge

potential to provide realistic and attractive application possibilities in integrated optical devices.

Planar waveguides with shorter waveguide length have the advantages of being smaller than the EDFA [28]. The rare-earth-doped waveguides contain various functions where its potential can not be found in the fibers type optical devices. These rare-earth doped silica optical waveguides can be used in integrating multiple optical devices (eg. optical source, circuit and amplifier) [29]. Both type of amplifier (fiber and planar) provide the same function but applicable under different condition; EDFA for long-haul transmission while EDWA for short distance transmission and integrated device. Therefore, it is unrealistic to establish any expectation that EDWA will completely replace EDFAs for high performance amplification in optical communication systems [8].

Studies on various kinds of Er-doped planar waveguides fabricated with different kind of host materials have been pursued in order to use them as amplifiers in the future optical communication systems. Silica-on-silicon EDWA has been the desirable goal since silica waveguides consist of similar composition as the optical fibers [29]. In addition, the use of silicon substrate also manage to simplify fiber connection [17].

1.4 EXISTING EDWAs FABRICATION TECHNOLOGIES

A variety of EDWAs fabrication techniques are available, as indicated in Table 1.2. FHD and PECVD are generally used in fabrication of EDWAs due to its high production rate. In this dissertation, erbium doped silica layer has been fabricated by FHD in conjunction with solution doping technique.

Table 1.2 Fabrication methods for EDWAs

Fabrication Methods	Type of EDWAs
Ion exchange	Silicate glass [30-33], Phosphate glass [34-41]
Ion implantation	SiO ₂ [42-43], SiON [44], Al ₂ O ₃ [45-46]
Electron beam evaporation	Silicate glass [47]
Sputtering	Silicate glass [48-51], Phosphate glass [52]
Solution/aerosol doping of FHD	Silica-on-silicon [16, 53-58]
Sol gel	Silica-on-silicon [17, 59-60]
PECVD	Phosphosilicate glass [61], Silica-on-silicon [62], Germanosilicate glass [63], Al ₂ O ₃ [64]

1.5 PROPOSAL OF THE STUDY

It has been a fortunate coincidence that erbium has the emission wavelength at 1550 nm which is compatible to the operating wavelength used in the fiber technology. This is why Er doped device become essentially important in the optical communication [14, 54]. In this dissertation, erbium is used as the primary dopant in sample preparation via solution doping. Because of rare-earth solubility limitation in silica matrix and clustering issue due to high doping concentration, co-dopants such as aluminium and ytterbium are suggested to be used.

The performance of the waveguide amplifier for a specific application is greatly dependent on the doping level. RE concentration in the waveguide can be controlled by suitable choice of soot composition, pre-sintered temperature (to control porosity) or increasing the RE solution concentration. In the present work, studies on the effect of solution concentration are placed as the priority and, soot composition and pre-sintered temperature has been judiciously selected. Experiment was designed to study RE incorporation with variation in co-dopant/RE ratio for either fixed RE concentration or co-dopant concentration in soaking solution. Apart from that, doping parameters such as doping period and doping cycle have also been varied and implemented in the experiment.

The objectives of this dissertation are as follow:

1. To determine the incorporation of RE into silica (glass)
2. To investigate the effects of different co-dopant
3. To investigate the effects of different solution's strength and method

1.6 THESIS OUTLINE

The beginning of Chapter 2 generally emphasized on the typical silicate glass structure and the bonding involved in the vitreous silica. B_2O_3 , GeO_2 and P_2O_5 are usually incorporated into silicate glass to improve the properties. Hence, the effect of these foreign atoms in altering the structure of silica matrices was discussed. Rare-earth plays the role as network-modifier in glass matrix and initially resulting in few common issues (low solubility, clustering, host selection) when impregnated into silica substrate. The solutions of the problems arose were briefly explained. Finally, the theory of the basic two or three level optical amplification was explained. Ytterbium co-doping compensate the ineffectiveness of amplification caused by cooperative up-conversion occurred in highly erbium doped samples.

In Chapter 3 an overview on the fabrication methods and principles are presented. The topic discussed here was basically on principles, methodology and mechanism involved in a flame hydrolysis deposition (FHD) system. After the preparation of FHD layer, sintering process took place. A porous medium was prepared at an adjustable pre-sinter temperature for solution doping. The solvent or solute used for solution doping determined the retention of rare-earth in silica glass. From the discussion, water (as solvent) and chloride salt (as solute) were used for solution doping. The methodology of solution doping was described precisely.

Chapter 4 elaborates on the result observed from the characterization using energy dispersive spectrometry (EDS), scanning electron microscopy (SEM) and prism coupler. In the first part, the morphology and microstructure of the samples prepared at various pre-sinter temperatures was discussed. Next, the relation between the full and half sintered erbium doped silica film was inspected. Then, the effect of erbium solution concentration on the erbium concentration in silica films was discussed. Under few circumstances, the effects of two different co-dopants (aluminium and ytterbium) on erbium doped silica films were analyzed. Multiple solution doping effects on the dopants concentration was discussed and the result was compared with the refractive index.

The overall result and future works was summarized in Chapter 5.

REFERENCES:

- [1] Hecht, J., "*Understanding Fiber Optics*". 4th ed. 2002. Upper Saddle River, N.J. USA: Prentice Hall.
- [2] Agrawal, G.P., "*Fiber-Optic Communication System*". 2nd ed. 1997. New York, USA: John Willey & Sons.
- [3] Spector, Andy, Sun, Jacob, and Eldada, Louay, "Title," unpublished|.
- [4] Watts, Samuel Pul, "Flame Hydrolysis Deposition of Photosensitive Silicate Layers Suitable for the Definition of Waveguiding Structures through Direct Ultraviolet Writing," PhD Thesis, Department of Electronics and Computer Science, University of Southampton, 2002.
- [5] Ramaswami, Rajiv and Sivarajan, Kumar N., "*Optical Network: A Practical Perspective*". 2nd ed. 2001. San Francisco, USA: Morgan Kaufmann.
- [6] Paul E. Green, Jr., "*Fiber To The Home The New Empowerment*".2006. Hoboken, New Jersey, Canada: John Wiley & Sons, Inc.
- [7] R.Simpson, Jay, "Rare Earth Doped Fiber Fabrication: Techniques and Physical Properties," in *Rare-earth-doped Fiber Lasers and Amplifiers*, Digonnet, Ed., 2 ed New York, USA: Marcel Dekker, Inc, 2001.
- [8] Bjarklev, Anders, "Optical Amplifiers," in *The Communications Handbook* Gibson, Ed., Second Edition ed Washington, DC: CRC Press, 2002.
- [9] Snitzer, E., "Proposed fiber cavities for optical lasers." *Appl. Phys.*, vol. 32 (1961) p. 36-39.
- [10] Koester, C. J. and Snitzer, E., "Amplification in a fiber laser." *Appl. Opt.*, vol. 3 (10), (1964) p. 1182.
- [11] Stone, J. and Burrus, C.A., "Nd-doped SiO₂ Lasers in end pumped fibre geometry." *Appl. Phys. Lett.*, vol. 23 (1973) p. 388-389.
- [12] Awagral, G.P., "*Nonlinear Fiber Optics*".1989. London: Academic Press.

- [13] Simon, J.C., "Semiconductor Laser Amplifier for Single Mode optical Fiber Communications." *J. Opt. Commun*, vol. 4 (2), (1983) p. 51-62.
- [14] Mears, R. J., Reekie, L., Jauncey, I. M., and Payne, D. N., "Low-noise erbium doped fiber amplifier operating at 1.54 μm ." *Electronics Letters*, vol. 23 (19), (1987) p. 1026.
- [15] Sidiroglou, F., Huntington, S., Roberts, A., and Baxter, G., "Micro-characterisation of erbium-doped fibers using a Raman confocal microscope." *Opt. Express* vol. 13 (14), (2005) p. 5506-5512.
- [16] Bonar, J. R. and Aitchison, J. S., "Co-doping effects in rare-earth-doped planar waveguides." *IEEE Proceedings Optoelectronics* vol. 143 (5), (1996) p. 293-297.
- [17] Huang, W. and Syms, R. R. A., "Sol-gel silica-on-silicon buried-channel EDWAs." *Journal of Lightwave Technology*, vol. 21 (5), (2003) p. 1339-1349.
- [18] Ziel, J. P., Bonner, W. A., Kopf, L., and Uitert, L., "Coherent emission from Ho^{3+} ions in epitaxially grown thin film aluminium garnet thin films." *Physics Letters*, vol. 42A (1), (1972) p. 105-106.
- [19] "Introduction to glass integrated optics".1992: Artech House.
- [20] Tien, P. K., "Integrated optics and new wave phenomena in optical waveguides." *Reviews of Modern Physics*, vol. 49 (2), (1977) p. 361-420.
- [21] Hunsperger, R., "Integrated Optics: theory and technology". 4th ed. 1995: Springer-Verlag.
- [22] Eggleston, J., Kane, T., Kuhn, K., Unternahrer, J., and Byer, R., "The slab geometry laser--Part I: Theory." *IEEE Journal of Quantum Electronics*, vol. 20 (3), (1984) p. 289-301.
- [23] Shepherd, D. P., Hettrick, S. j., Li, C., Mackenzie, J. I., Beach, R. J., Mitchell, S. C., and Meissner, H. E., "High-power planar dielectric waveguide lasers." *Physics D: Applied Physics*, vol. 34 (2001) p. 2420-2432.

- [24] Adikan, Faisal Rafiq Mahamd, "Direct UV-written waveguide devices," Faculty of Science, Engineering & Mathematics Optoelectronics Research Centre, University of Southampton, June 2007.
- [25] Sun, C. Jacob, Schmidt, Kevin M., and Lin, Wenhua, "Silica waveguide devices and their applications," in *Photonics West 05*, San Jose, CA, USA, 2005, p. 9-17.
- [26] Ro, Sung Ing, Jung, TYong Soon, and Shin, Dong Wook, "The effects of Er/Al co-doping on the fluorescence of silica waveguide film." *Journal of Ceramic Processing Research*, vol. 2 (4), (2001) p. 155-159.
- [27] Shimizu, M., Yamada, M., Horiguchi, M., and Sugita, E., "Concentration effect on optical amplification characteristics of Er-doped silica single-mode fibers." *IEEE Photonics Technology Letters*, vol. 2 (1), (1990) p. 43-45.
- [28] Hattori, K., "Er-doped planar waveguide devices," in *IEEE Lasers and Electro-Optics Society Annual Meeting, 1997. LEOS '97 10th Annual Meeting. Conference Proceedings.*, 1997, p. 308-309.
- [29] Hibino, Y., Kitagawa, T., Shimizu, M., Hanawa, F. A. Hanawa F., and Sugita, A. A. Sugita A., "Neodymium-doped silica optical waveguide laser on silicon substrate." *IEEE Photonics Technology Letters*, vol. 1 (11), (1989) p. 349-350.
- [30] Feuchter, T., Mwarania, E. K., Wang, J., Reekie, L., and Wilkinson, J. S., "Erbium-doped ion-exchanged waveguide lasers in BK-7 glass." *IEEE Photonics Technology Letters*, vol. 4 (6), (1992) p. 542-544.
- [31] Zheng, X. H. and Mears, R. J., "Planar optical waveguides formed by erbium ion exchange in glass." *Appl. Phys. Lett.*, vol. 62 (1993) p. 793-795.
- [32] Roman, J. E., Camy, P., Hempstead, M., and Wilkinson, W. S., "Ion-exchanged Er/Yb waveguide laser at 1.5 μm pumped by laser diode." *Electronics Letters*, vol. 31 (1995) p. 1345-1346.

- [33] Camy, P., Roman, J. E., Willems, F. W., Hempstead, M., Plaats, J. C. van der, Prel, C., Beguin, A., Koonen, A. M. J., and Wilkinson, J. S., "Ion exchanged planar lossless splitter at 1.5 μm ." *Electronics Letters*, vol. 32 (1996) p. 321-323.
- [34] Honkanen, S., Najafi, S. I., Poyhonen, O., Orsel, G., Wang, W. J., and Chrostowski, J., "Silver-film ion-exchanged single-mode waveguides in Er-doped phosphate glass." *Electronics Letters*, vol. 27 (1991) p. 2167-2168.
- [35] Ohtsuki, T., Peyghambarian, N., Honkanen, S., and Najafi, S. I., "Gain characteristics of a high concentration Er³⁺-doped phosphate-glass waveguide." *J. Appl. Phys.*, vol. 78 (1995) p. 3617-3621.
- [36] Fournier, P., Meshkinfam, P., Fardad, M. A., Andrews, M. P., and Najafi, S. I., "Potassium ion-exchanged Er-Yb doped phosphate glass amplifier." *Electronics Letters*, vol. 33 (4), (1997) p. 293-295.
- [37] Shoostari, A., Meshkinfam, P., Touam, T., Fardad, M. A., Andrews, M. P., and Najafi, S. I., "Potassium ion-exchanged Er/Yb doped phosphate glass amplifier." *Electronics Letters*, vol. 34 (1998) p. 704-705.
- [38] Veasey, D. L., Funk, D. S., Peters, P. M., Sanford, N. A., Obarski, G. E., Fontaine, N., Young, M., Peskin, A. P., Liu, W. C., Walter, S. N. Houde, and Hayden, J. S., "Yb/Er codoped and Yb doped waveguide lasers in phosphate glass." *Non-crystalline Solids*, vol. 263 (369-381), (2000)
- [39] Delavaux, J. M. P., Granlund, S., Mizuhara, O., Tzeng, L. D., Barbier, D., Rattay, M., Andre, F. Saint, and Kevorjian, A., "Integrated optics erbium-ytterbium amplifier system in 10-Gb/s fiber transmission experiment." *IEEE Photonics Technology Letters*, vol. 9 (1997) p. 247-249.
- [40] Barbier, D., Rattay, M., Andre, F. Saint, Clauss, G., Trouillon, M., Kevorkian, A., P. Delavaux, J. M., and Murphy, E., "Amplifying four-wavelength combiner,

- based on erbium/ytterbium-doped waveguide amplifiers and integrated splitters." *IEEE Photonics Technology Letters*, vol. 9 (1997) p. 315-317.
- [41] Jaouen, Y., Mouza, L. du, Barbier, D., Delavaux, J. M. P., and Bruno, P., "Eight-wavelength Er-Yb doped amplifier: Combiner/splittter planar integrated module." *IEEE photonics Technology Letters*, vol. 11 (1999) p. 1105-1107.
- [42] Polman, A., Lidgard, A., Jacobsen, D. C., Becker, P. C., Kistler, R. C., Blonder, G. E., and Poate, J. M., "1.54 μm room temperature luminescence of MeV erbium ion implanted silica glass." *Appl. Phys. Lett.*, vol. 57 (1990) p. 2859-2861.
- [43] Ligard, A., Polman, A., Jacobsen, A., Blonder, G. E., Kistler, R., Poate, J. M., and Becker, P. C., "Fluorescence lifetime studies of MeV erbium implanted silica glass." *Electronics Letters*, vol. 27 (1991) p. 993-995.
- [44] Chelnokov, A. V., Lourtioz, J. M., Boucard, Ph., Bernas, H., Chaumont, J., and Plowman, T., "Deep high-dose erbium implantation of low-loss silicon oxynitride waveguides." *Electronics Letters*, vol. 30 (1994) p. 1850-1852.
- [45] Hoven, G. N. van der, Koper, R. J. I., Polman, A., Dam, C. van, Uffeien, J. W. M. van, and Smit, M. K., "Net optical gain at 1.53 μm in Er doped Al_2O_3 waveguides on silicon." *Appl. Phys. Lett.*, vol. 68 (1996) p. 1886-1888.
- [46] Snoeks, E., Hoven, G. N. van den, and Polman, A., "Optimization of an Er-doped silica glass optical waveguide amplifier." *IEEE Journal of Quantum Electronics*, vol. 32 (1996) p. 1680-1684.
- [47] Nagazawa, M. and Kimura, Y., "Electron-beam vapor-deposited erbium-doped glass waveguide laser at 1.53 μm ." *Electronics Letters*, vol. 28 (1992) p. 2054-2056.

- [48] Schmulovich, J., Wong, A., Wong, Y. H., Becker, P. C., Bruce, A. J., and Adar, R., "Er³⁺ glass waveguide amplifier at 1.55 μm on silicon." *Electronics Letters*, vol. 28 (1181-1182), (1992)
- [49] Nykolak, G., Becker, P. C., Schmulovich, J., DiGiovanni, Y. H. Wong D. J., and Bruce, A. J., "Concentration-dependent I_{4(13/2)} lifetimes in Er³⁺-doped fibers and Er³⁺-doped planar waveguides." *IEEE Photonics Technology Letters*, vol. 5 (1993) p. 1014-1016.
- [50] Nykolak, G., Haner, M., Becker, P. C., Schmulovich, J., and Wong, Y. H., "Systems evaluation of an Er³⁺ -doped planar waveguide amplifier." *IEEE Photonics Technology Letters*, vol. 5 (1993) p. 1185-1187.
- [51] Ghosh, R. N., Schmulovich, J., Kane, C. F., Barros, M. R. X. de, Nykolak, G., Bruce, A. J., and Becker, P. C., "8-mW threshold Er³⁺ -doped planar waveguide amplifier." *IEEE Photonics Technology Letters*, vol. 8 (1996) p. 518-520.
- [52] Yan, Y. C., Faber, A. J., Waal, H. de, Kik, P. G., and Polman, A., "Erbium-doped phosphate glass waveguide on silicon with 4.1 dB/cm gain at 1.535 μm ." *Appl. Phys. Lett.*, vol. 71 (1997) p. 2922.
- [53] Bebbington, J. A., Barbarossa, G., Bonar, J. R., and Aitchinson, J. S., "Rare-earth doped silica waveguides on Si fabricated by flame hydrolysis deposition." *Applied Physics Letters*, vol. 62 (4), (1993) p. 337-339.
- [54] Kitagawa, T., Hattori, K., Shimizu, M., Ohmori, Y. A. Ohmori Y., and Kobayashi, M. A. Kobayashi M., "Guided-wave laser based on erbium-doped silica planar lightwave circuit." *Electronics Letters*, vol. 27 (4), (1991) p. 334-335.
- [55] Kitagawa, T., Hattori, K., Shuto, K., Yuso, M., Kobayashi, M., and Horiguchi, M., "Amplification in erbium-doped silica-based planar lightwave circuits." *Electronics Letters*, vol. 28 (1992) p. 1818-1819.

- [56] Hattori, K., Kitagawa, T., Oguma, M., Wada, M., Temmyo, J., and Horiguchi, M., "Erbium-doped silica-based planar waveguide amplifier pumped by 0.98 μm laser diodes." *Electronics Letters*, vol. 29 (1993) p. 357-359.
- [57] Hattori, K., Kitagawa, T., Oguma, M., Ohmori, Y., and Horiguchi, M., "Erbium-doped silica based waveguide amplifier integrated with a 980/1530nm WDM coupler." *Electronics Letters*, vol. 30 (11), (1994) p. 856-857.
- [58] Maxwell, G. D., "Photosensitivity and rare earth doping in flame-hydrolysis-deposited planar silica waveguides," in *Proc. SPIE*, 1996, p. 16-29.
- [59] Yang, L., Saavedra, S., Armstrong, N. R., and Hayes, J., "Fabrication and characterization of low-loss, sol-gel planar waveguides." *Anal. Chem.*, vol. 66 (1994) p. 1254-1263.
- [60] Thomson, R. R., Bookey, H. T., Ur-Rehman, H., Liu, S., Suyal, N., and Kar, A. K., "Optically active erbium-doped waveguides fabricated using a single-sol-gel-deposition technique." *Journal of Lightwave Technology* vol. 23 (12), (2005) p. 4249-4256.
- [61] Shuto, K., Hattori, K., Kitagawa, T., Ohmori, Y., and Horiguchi, M., "Erbium-doped phosphosilicate glass waveguide amplifier fabricated by PECVD." *Electronics Letters*, vol. 29 (1993) p. 139-141.
- [62] Pederson, B., Fuchter, T., Polsen, M., Pesersen, J. E., Kristensen, M., and Kromann, R., "High concentration erbium doped silica-on-silicon grown by plasma enhanced CVD," in *Proc ECIO'95*, Delft, The Netherlands, 1995.
- [63] Guldborg-Kjaer, S., Hubner, J., Kristensen, M., Laurent-Lund, C., Rysholt Poulsen, M., and Sckerl, M. W., "Planar waveguide laser in Er/Al-doped germanosilicate." *Electronics Letters*, vol. 35 (4), (1999) p. 302-303.

- [64] Chryssou, C. E. and Pitt, C. W., "Er³⁺ -doped Al₂O₃ thin films by plasma enhanced chemical vapor deposition (PECVD) exhibiting a 55-nm optical bandwidth." *IEEE Journal of Quantum Electronics*, vol. 34 (1998) p. 282-285.

CHAPTER 2

INTRODUCTION TO GLASS

Glass is an amorphous material which is formed through rapid cooling of its liquid phase material such that crystallization is prohibited. The main component found in many glasses is the most abundant mineral in the earth's crust - silica (silicon dioxide). Silica is one of the most versatile substances on earth that is very much applicable in a variety of forms due to its excellent properties; chemical interactions resistance, extremes heat and cold sustainability, and recyclable. Therefore, glass is suitably applicable in variety of field: from the ordinary flat glass, container glass, laboratory equipment, thermal insulator, reinforcement fiber to the optics and optoelectronics material.

Ordinary silica glass normally contains impurities (eg. metallic ions) which contribute to loss greater than 100dB km^{-1} due to absorption. However, the requirement for a low transmission loss glass in an optical device is essential. Pure glass has withstood such requirement; its loss is remarkably low that is below 1dB km^{-1} at infrared wavelengths between 1.0 and 1.8 microns [1]. Over the decades, pure glass has been well recognized in the optical devices fabrication due to its very low loss transmission characteristic at the transmission window.

Glass substrates for integrated optics are used in certain application such as telecommunications because they have high availability, relatively low cost and contain a refractive index that is naturally matched to silica optical fibers [2].

2.1 GLASS STRUCTURE

Contrary to the crystalline materials, glass shows lack of uniformity and symmetry, and had no regular atomic arrangement and long-range-periodicity [3]. In fact, glass consist of short-range order with a three-dimensional polyhedron structure (Figure 2.1), commonly a tetrahedron [4]. Excluding silica, non-metal elements in groups 13, 14 and 15 (Refer Figure 2.2) are among the important glass-forming elements. These elements can combine with oxygen to form oxide glass. More precisely, the oxide glass is the result of three-dimensional network formation along with oxygen [5], which is covalently bonded with strong and directional bonds [4].

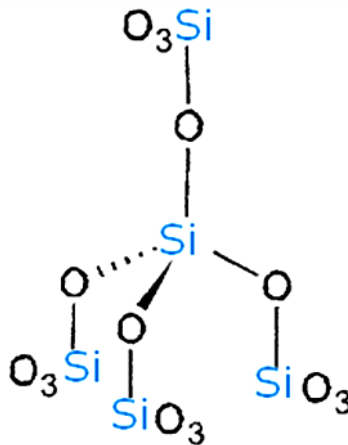


Figure 2.1 Chemical structure of silica matrix [6].

The simplest oxide glass comprises of two elements; glass-forming atom and oxygen. Oxides like SiO₂, B₂O₃, GeO₂ and P₂O₅ are the basic glass-former that satisfy the condition stated by Zachariasen's rules for glass formation [3]. Besides, combining different oxides for multi component structure is possible by modifying the basic composition. This can be done either by introducing a modifier atom for basic structure alteration or adding an element for glass-former atom replacement. These oxides structure formed is well considered by Zachariasen; who have not only suggested about empirical observations for oxides but also predicted those oxides that tend to form glass.

According to the rules of Zachariasen for glass formation, no oxygen atom can be linked to more than two glass-forming atoms. The glass-forming ions coordination number must be small: 3 or 4 and oxygen polyhedral must only share corners and not edges or faces. Apart from that, polyhedral must form a three-dimensional network.

The implication brought from the above rules show that glass formation is more likely with open and low density polyhedral structures; hence not all oxides (eg. MgO, Al₂O₃ and CaO) are suitable in glass formation.



Figure 2.2 Periodic table.

Figure 2.3(a) shows the vitreous silica (SiO_2) is the common glass structures. Silicon atom in the centre is covalently bonded with four oxygen atoms which arranged in tetrahedral form. Obeying the Zachariasen's third rule, each of this tetrahedron is silicon-oxygen bonded to another four tetrahedrons by only sharing corners. The structure formed almost resembles the crystalline structure of silica or known as cristobalite (Figure 2.3(b)), though it is in random form which results in lack of long-range periodicity, uniformity and symmetry.

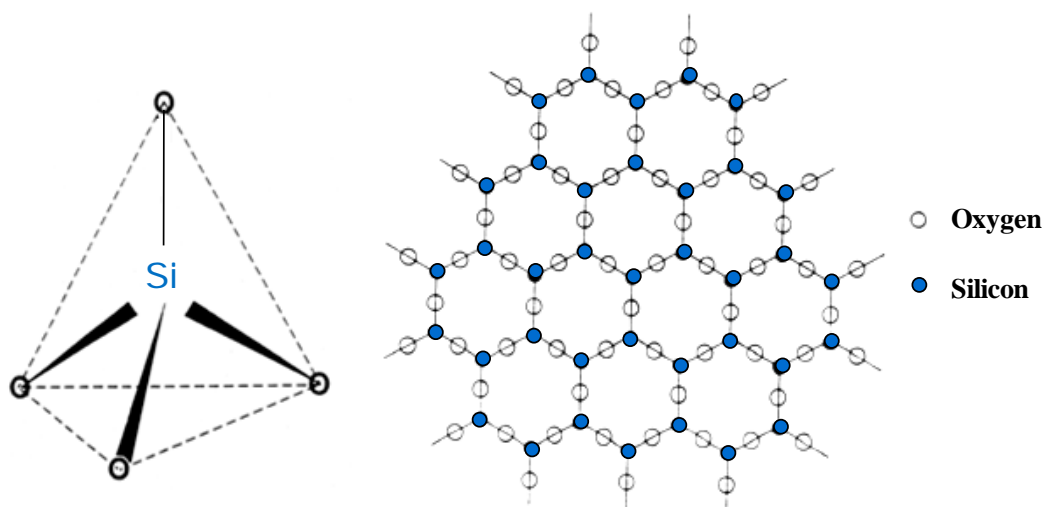


Figure 2.3 (a) Schematic of three-dimensional tetrahedral arrangement in fused silica glass; (b) Two-dimensional arrangement of silicon and oxygen atoms in cristobalite [5].

It is essential to know that even in pure glass, not all oxygen atoms are found to link to other tetrahedron. Some oxygen atoms might escape from the linkage - termed as non-bridging atoms. Normally, the existence of non-bridging oxygen atoms in pure silica might be very few [7]. These non-bridging oxygen atoms tend to bond with other species (eg. network-modifying elements) via ionic bonding.

Network-modifying elements are capable of adjusting the connectivity and dimensionality of the glass network by forming ionic and non-directional bonds which is considered as weak bonding [8-9]. These network-modifying elements tend to be from group 1, 2 or the lanthanides of the periodic table (refer Figure 2.2); the introduction of network-modifying elements will lead to the disruption of glass structure where silicon-oxygen structure is opened up (refer Figure 2.4). Hence, the properties of the glass would have changed: density of the glass is lowered, bond strength is weakened and both the fusion temperature and viscosity of the glass is lowered.

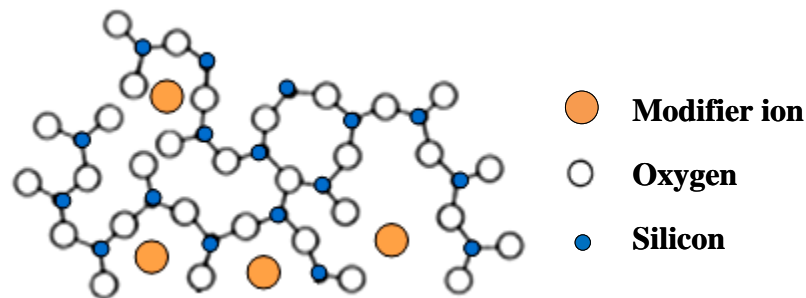


Figure 2.4 Schematic of a disrupted silica glass structure by addition of modifier ions [5].

Some of the oxygen bridging atoms might encounter breakage, thus increasing the number of non-bridging oxygen atoms. These oxygen ions are negatively charged and therefore can be used to compensate the positively charged of the network-modifying elements. However, according to the ‘continuous-random-network’ (CRN) theory [3, 10], the modifiers encounter difficulty in spreading uniformly throughout the glass; it is instead distributed non-randomly and inhomogeneously in glass. This lead to clustering among modifier-rich regions or glass-former-rich region separation [11].

Network modifiers are also known as the active element doped in the glass and this will be further elaborated in Section 2.2. In the typical oxide glass fabrication for optical devices, network-forming elements other than Si such as Ge, P and B are also included. Each of these elements reacts and contributes differently in altering the structure of silicon oxide glass.

2.1.1 GERMANOSILICATE GLASS

Germanium itself forms a fully bridging tetrahedral structure like silicon. The addition of germanium in silica matrix results in a simple substitution of Ge atom over silicon atom (refer Figure 2.5). The properties remain nearly the same as the fused silica glass only if the tetrahedral structure is retained [12]. However, such substitution might cause stress to the matrix due to the difference in bond length and bond angle: the Ge-O bond length is ~8% longer than the Si-O bond and Ge-O-Ge bond angle is 133° while the Si-O-Si bond angle is 144° . The stress applied within the matrix tends to affect the physical properties of the glass and hence, increases the chance of defects occurring within the structure [13].

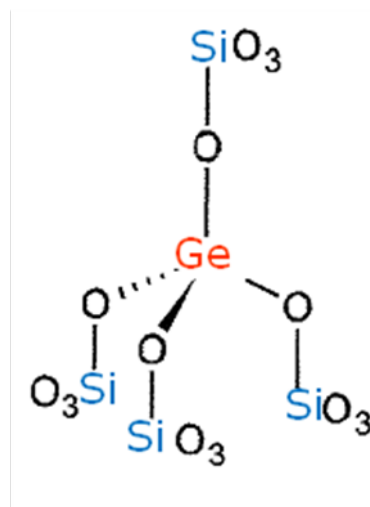


Figure 2.5 Inclusion of Ge atom within silica matrix [6].

Germanosilicate glasses encounter disordering effect and are weaker matrix compared to pure silica; this is why the melting point and glass transition temperature are decreased. Meanwhile, the refractive index of silicate glass increases if germanium doping level increases. This is closely related to the “tighter” bonds formed under a relatively higher stress, resulting in an increment in deep UV adsorption. Germanium doping is found widespread both in the fields of fiber and planar optics. Its application not only includes in reducing melting point and increasing refractive index but also play a part in photosensitivity for optical purposes [13].

2.1.2 PHOSPHOSILICATE GLASS

In phosphate glass system, each phosphorus atom is bonded covalently to four oxygen atoms [12]. One of the oxygen atoms from the tetrahedron remains non-bridging due to the pentavalent nature of the P ion (refer Figure 2.8) [13]. In other word, one of the oxygen is double bonded to the phosphorus as phosphorus contains a valency of 5. Therefore, there are only three oxygen left that can bond with other species. This eventually makes the phosphate glass less dense than the silica glass.

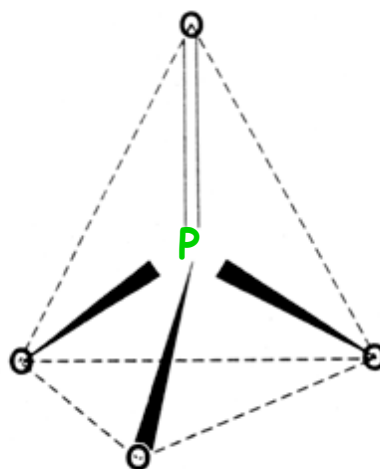


Figure 2.6 Schematic of three-dimensional tetrahedral arrangement for phosphate glass; showing double bond between one oxygen and the phosphorus [5].

Normally, phosphorus is incorporated as co-dopant in silica to produce phosphosilicate glasses $\text{SiO}_2: \text{P}_2\text{O}_5$. The PO_4 tetrahedron will be substituted into the silica matrix (refer Figure 2.7). The existence of non-bridging oxygen atoms within the silica matrix might cause termination of chain structures. Hence, formation of isolated chains is possible through P doping and this normally does not occur in clear pure silica. Phosphosilicate glasses are considered significantly less rigid structurally and this resulted in the decreasing of both melting points and glass transition temperatures as compared to pure silica [13]. Phosphorus can be used with fluorine to be incorporated into silica glass such that sintering temperature is lowered while the refractive index remain the same [14]. The sintering temperature is affected by the viscosity of the silica and it can be lowered with just adding in a small amount of phosphorus to the silica network.

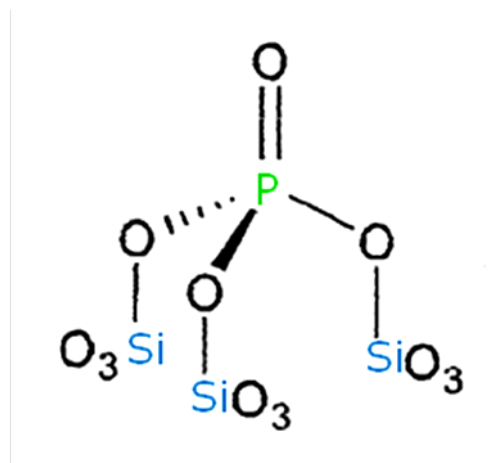


Figure 2.7 Inclusion of P atom within a silica matrix [6].

The effect of P_2O_5 in SiO_2 can be elaborated based on the $\text{P}_2\text{O}_5:\text{SiO}_2$ phase diagram shown in (refer Figure 2.8). The liquidus line is being affected as phosphorus concentration varies and the eutectic point falls on ~ 20 mole% P_2O_5 . Though, a doping level of ~ 10 mole% P_2O_5 is sufficient to approach the target for a lower melting point of ~ 1200 °C [13].

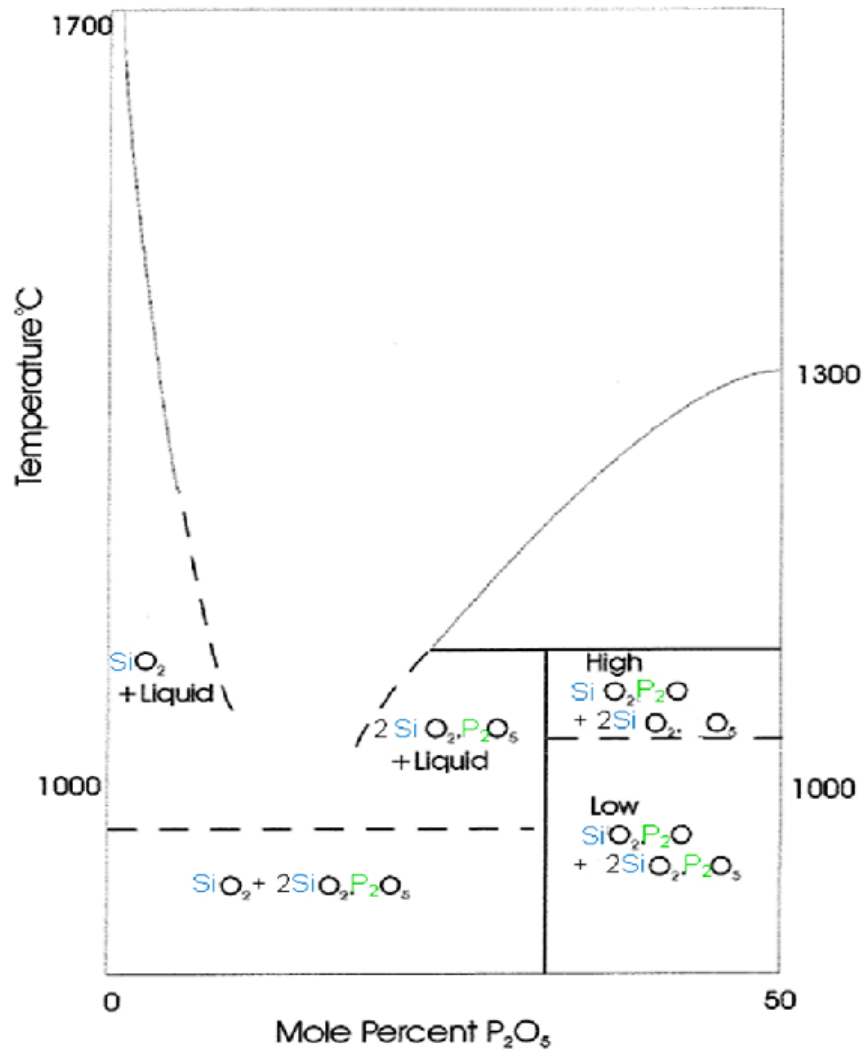


Figure 2.8 Phase diagram representing Phosphorus doping of silica [15]

According to the Kramers-Kronig relationship [16], an increased absorption in the ultraviolet leads to a higher refractive index. The refractive index of a medium is eventually related to the absorption in the deep UV when considering the spectral absorption from zero to infinite frequencies [13]. Therefore, the refractive index of the doped silica glass increases as phosphorus doping level increases (refer Figure 2.9). Phosphosilicate glasses are well recognized in the field of fiber and planar optics as such glasses are easily produced and chemically stable.

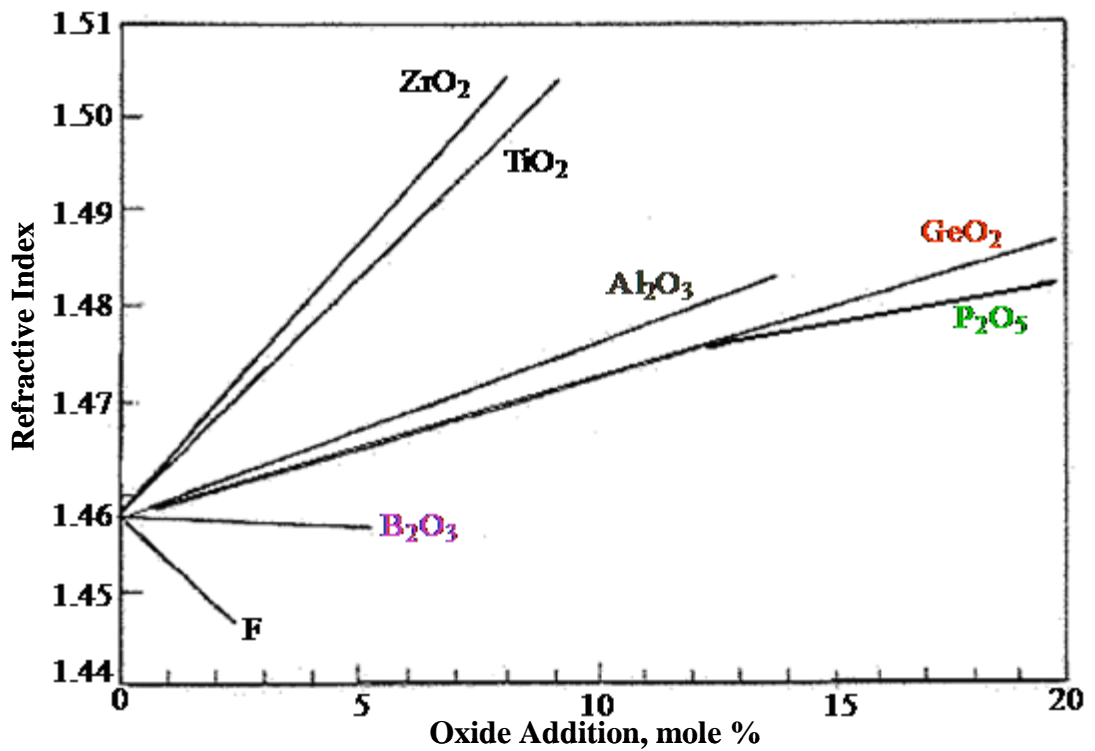


Figure 2.9 Effect of dopants upon refractive index at 598 nm [17].

2.1.3 BOROSILICATE GLASS

The basic building block of borate glass is B_2O_3 where boron forms three bonds with oxygen atoms. In a two-dimensional planar ring for borate glass (refer Figure 2.10), boron and oxygen atoms are found linking together via bridging oxygen atoms [12, 18].

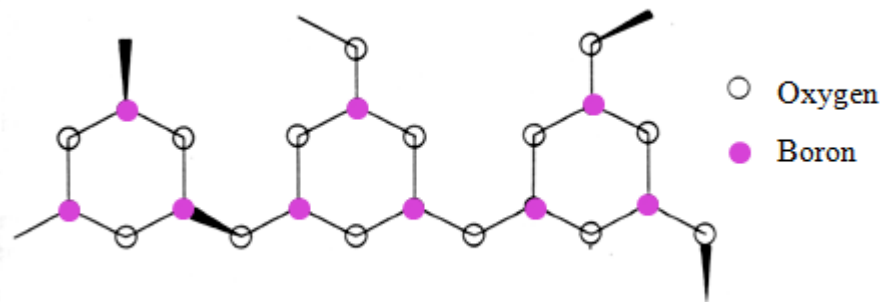


Figure 2.10 Two-dimensional arrangement of boron and oxygen atoms in borate glass [5].

Incorporation of boric oxide, B_2O_3 into silica matrix will form borosilicate glasses (refer Figure 2.11). Since three oxygen atoms coordinate with one boron atom, this results in a triangular structural unit consisting of BO_3 . The B atom is believed to posit slightly above the plane of three bridging oxygen atoms [6].

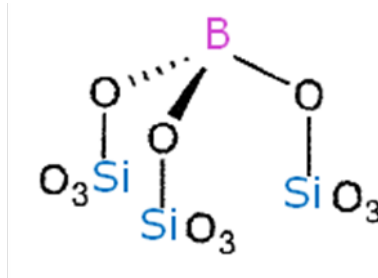


Figure 2.11 Inclusion of B atom within silica matrix [6].

The structure formed displays similar effects as the addition of phosphorus into silica; both provide three bridging oxygen atoms. The interconnected structure becomes noticeably less as BO_3 acts as terminators in silica matrix. As a result, the borosilicate glass formed is less rigid and display a lower melting point and glass transition temperature as compared to pure silica. Apart from that, boron doping has shown a different effect even though it is relatively slight compared to other dopants; the refractive index decreases as the doping level increases [13].

Boron is not suitable in long wavelength telecoms application as it contains very short phonon edge ($\sim 7 \mu\text{m}$) [19-20]. Due to this matter, boron is rarely used in large amount in the modern low loss fiber as its relatively low wavelength of fundamental absorption ($7.2 \mu\text{m}$) can affect attenuation within 1300-1550 nm wavelength range used in telecommunications systems. Furthermore, the high amount of boron addition also increase the effect of overtones present within the telecoms window [13]. In spite of this, boron doping of silicate glasses has found to be widespread in planar optics.

2.2 ACTIVE ELEMENT DOPED GLASS

Rare-earth ions have a long history in optical applications particularly in luminescent devices using single crystals, powders and glasses. Rare-earths consist of few important characteristics that make them distinguishable from other optically active ions. Firstly, rare-earths emit and absorb over narrow ranges of wavelength. Secondly, the intensities of the emission and absorption transitions are weak and its wavelengths are relatively insensitive to host material. The preceding characteristics are due to the fact that the electron of rare-earth is more favorable to fill the outer lying $5s$ and $5p$ electron shells than the inner $4f$ electron shells [21]. The outer layer acts as a shield for the $4f$ electrons such that absorption and emission characteristic of the ion is not affected when doped in different host [22]. In addition, the lifetimes of rare-earth's metastable states are long and its quantum efficiencies tend to be high. All of these properties brought to the excellent performance of rare-earth ions in vulnerable optical applications [23] especially in amplification [24].

As discussed earlier, rare-earth plays the role as network modifier when incorporated into glass matrix where the covalently bonded glass structure is being broken up [5, 25]. Hence, non-bridging oxygen atoms are formed and required charge compensation. There are two conditions to be considered: under a low rare-earth concentration, the ions will be in an isolated site; do not receive much influence from other rare-earth ions. Meanwhile, if rare-earth is doped above a critical concentration, the rare-earth ions become closer and might bring to concentration quenching for certain rare-earth ions. Moreover, the host glass selection is also crucial as it could give a great impact on the stability of rare-earth ions in glasses [5, 26]. This is because different network modifiers show different solubility in certain type of glass.

2.2.1 LOW SOLUBILITY

Low solubility of rare-earth dopant might affect the fluorescence lifetime, absorption, emission and excited state absorption cross sections of the dopant transitions. Such low solubility of rare-earth ions in glass is caused by the tetrahedron structure of the silica and its low number of non-bridging oxygen atom. This is due to lack amount of the rare-earth's matching charge for the coordination to the silica matrix [7]. To overcome such implication, the solubility of the rare-earth in silica has to be improved and this simply means to increase the number of non-bridging oxygen atom in silica. This can be approached by inclusion of alkali-metals or aluminium as co-dopant to silica [7, 27].

Aluminium oxide is an intermediate type of element so it could not easily form a glass independently [28]. Though, aluminium ions can be impregnated in the silica matrix either as 'network formers' via tetrahedral coordination or as 'network modifiers' via hexahedral coordination, depending on the aluminium concentration [29-30]. However, the incorporation of aluminium into silica glass by substituting some silica ions led to charge imbalance. This is because aluminium oxide as trivalent ion required charge compensation to approach charge equity. The charge deficiency of aluminium tends to be balanced up by positively charged rare-earth ions. It is believed that rare-earths are preferable to congregate on the aluminium sites forming Al-O-RE when being introduced in an $\text{Al}_2\text{O}_3\text{-SiO}_2$ glass [9, 31].

Not only improving the solubility, aluminium has also been used as a new alternative to germanium for increasing the refractive index of the core layer in the fiber for telecommunication [32]. Investigation based on power amplifier [33-34] and small-signal amplifier [35] for Ge-doped silica have indicated that quenching did appear.

Therefore, expectation is made such that Ge does not contribute sufficiently in the tetrahedral silica network alteration for improving the rare-earth ions solubility [9].

In standard telecommunications fiber, germanium (5.0 mol% GeO_2) and phosphorus (0.5mol% P_2O_5) as the index raising dopants are used to modify the silica structure; the incorporation of Nd is limited to about 1000 ppm right before fluorescence quenching occurs [36]. To improve the solubility of rare-earth ions in silica, aluminium oxide is impregnated as the network modifier [36-41]. Fiber host compositions with 8.5 mol% Al_2O_3 have been claimed to successfully doped with 2% of rare-earth concentration [40].

Regarding to the incorporation of aluminium oxide (Al_2O_3) for increase solubility, using neodymium oxide (Nd_2O_3) as an example; Arai et al. has stated that Nd_2O_3 dissolves in Al_2O_3 and not in SiO_2 whereas Al_2O_3 dissolves in SiO_2 . This somehow shows the role of Al_2O_3 to form a solvation shell around the rare-earth ion, and initially prepare the rare-earth ion for incorporation in silica network. In this case, the ratio of Al and Nd have to be small (~ 10) to prevent clustering [39].

2.2.2 CLUSTERING

Rare-earth clustering or aggregation is a critical issue found during rare-earth impregnation in silica substrate and it is believed that several factors have contributed to such manner. The forces (eg. ionic forces) that make the particle cluster together, the time the particles are free to move, the concentration and also the speed of the particles [7]. Hence, the forming condition of the particles has to be well adjusted in order to achieve homogeneous rare-earth incorporation in silica.

Pure silica can incorporate only very small amounts of rare-earths before microscopic clustering occurs and interactions of ion-ion appear. Crystalline phases may form beyond certain concentration if it is high enough [36]. In the rigid silica network, the number of non-bridging oxygen atoms is found to be insufficient to coordinate isolated rare-earth since rare-earth ions require large coordination numbers. This eventually causes clustering as the rare-earth ions gather to share the non-bridging oxygen [39].

Clustering issue is considered closely related to the solubility of rare-earth itself in silica matrix. Again, aluminium was used to alleviate in the solubility problem. Rare-earth ions are preferably to aggregate near Al^{3+} and form Al-O-RE rather than agglomerate to form RE-O-RE [9]. This phenomenon subsequently causes a larger spacing among rare-earth elements. Hence, it is believed that the presence of aluminium is also helpful in suppressing the clustering of the rare-earth ions in silica host [27, 42].

Clustering is often found when doped above a critical concentration leading to degradation in device performances due to unwanted scattering loss, rapid fluorescent decay and quenching of laser emission [39]. Based on the luminescence decay data, the Nd concentration that led to clustering in pure silica was estimated to be about 10^{19} cm^{-3} [43]. Meanwhile, Er ion-ion interactions have been significantly revealed at the levels which is approximately 10^{18} cm^{-3} [44].

2.2.3 HOST MATERIAL

Host selection is critical in affecting the excited-state absorption for a given rare-earth ion transition. It has been demonstrated that there is decrement in the excited-state absorption in erbium-doped fibers for a germanosilicate host compared to an aluminosilicate host [39]. Rare-earth stands the chance in contributing to the background losses due to impurity absorption and scattering mechanisms and this might decrease the efficiency of the fiber device. During the process of distributing gain along the amplifiers, pump light ought to travel long distances and internal loss tend to occur. The magnitude of the internal loss has been calculated for a 50 km distributed amplifier with a near-optimum Er dopant level for transparency. Results show an increment in the background loss from 0.2 to 0.3 dB km⁻¹ and point to a fivefold increment in the required pump power [45]. Therefore, the background loss for a distributed amplifier must be low enough to be kept near the fusion splice losses such that the reduction in performance is minimized.

The main challenge in the fabrication of rare-earth silica waveguide is approaching the efficiency in incorporating the dopants into glass. All of the issues mentioned above can affect the doping efficiency and bring significant influence on the optical device.

High rare-earth concentration is a must in order to achieve sufficient absorption for the required high output powers [5]. The capability for host glass in sustaining a relatively high concentration of rare-earth without clustering require the open, chain-like structure of phosphate glass or by addition of modifier ions (Ca, Na, K, Li etc.) to open silicate structure and thus increase solubility [46-48].

2.3 OPTICAL AMPLIFICATION

Generally, pumping is done by radiation of laser diode that supplies a powerful light at a wavelength other than the wavelength of the information signal. Together with the optical information, optical pumping beams are put in the same active medium using a coupler. Both of those two beams propagate along the rare-earth doped medium such that the information signal is amplified while the pumping signal encounter power losses [49].

2.3.1 THEORY OF OPTICAL AMPLIFICATION

Amplification in an optical amplifier is based on the stimulated emission mechanism. First of all, pumping signal provides energy that is adequate for rare-earth ions excitation at the upper energy band. Such excitation is done when rare-earth ions absorb photon produced by the pump laser. Then, stimulated by the information signal, these excited ions tend to encounter a lower energy band transition. Such transitions result in the radiation of photons with the same energy consist the same wavelength, direction, and phase as the input signal has [49].

Free ions of rare-earth exhibit discrete energy levels. The energy levels of rare-earth ions in silica medium are split into a number of closely related levels namely energy band. These energy bands not only provide the amplifier the ability to amplify more than one wavelength but also eliminate the need to fine-tune a pumping wavelength [49].

The purpose of pumping is to achieve population inversion; meaning having more ions of dopant at the intermediate level (level 2) than at the lower level (level 1). Therefore, dopant ions are pumped to the intermediate level in order to attain population

inversion. In a typical Er-doped amplifier, pumping can be achieved either by a direct pumping at 1480 nm wavelength or indirect pumping at 980 nm wavelength [49].

2.3.2 AMPLIFICATION IN 2-LEVEL AND 3-LEVEL SYSTEMS

Two energy levels system are established when pumping is done directly by using a 1480 nm wavelength source. Such pumping, normally by external optical energy (at 1480 nm) will take the Er ions from the lower level (level 1) to the intermediate level (level 2). The lifetime of Er ions at this intermediate level is long enough for accumulation of ions to occur, and hence, creating population inversion. These Er ions will eventually fall to the lower level (level 1), radiating the desired wavelength [49].

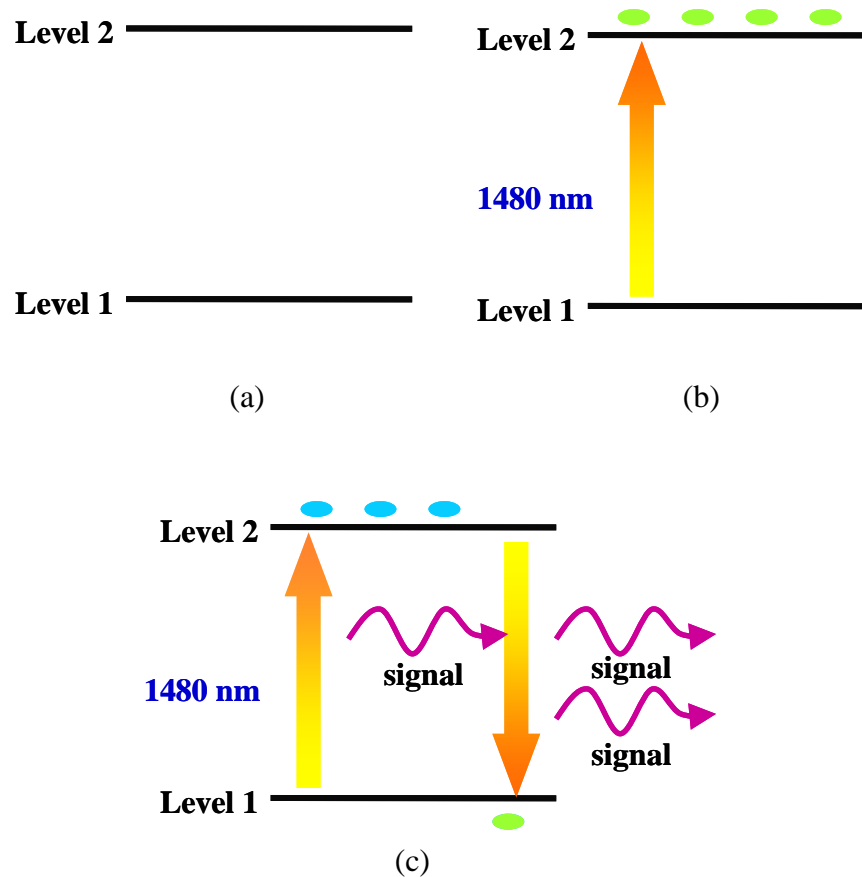
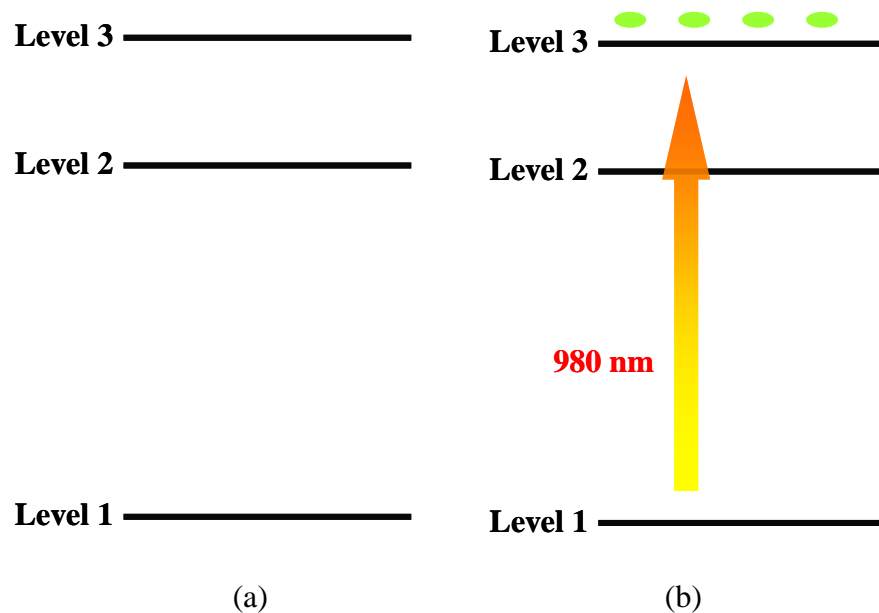


Figure 2.12 Two-level amplification system. (a) RE at rest, (b) lower case pumping by external optical energy, (c) emission by stimulation.

In a 3 level system, indirect pumping method are applied where 980 nm pumping source is used to move the rare-earth ions from the lower state to the upper level (level 3) in a continuous manner. There, these ions will decay non-radiatively to the intermediate energy level (level 2); then, follow by falling to the lower level (level 1) where the desired wavelength of 1550 to 1600 nm is being radiated. The lifetime of Er ions at the upper level (level 3) is about 1 μ s. Meanwhile, the Er ions at the intermediate level (level 2 or also known as metastable level) has longer lifetime and it is approximately greater than 10 ms. This means that Er ions pumped at the upper level encounter rapid non-radiative relaxation that descend to the intermediate level (level 2), and stay at that level for relatively long time. Therefore, population inversion has been created due to Er ions accumulation at the intermediate level [49].



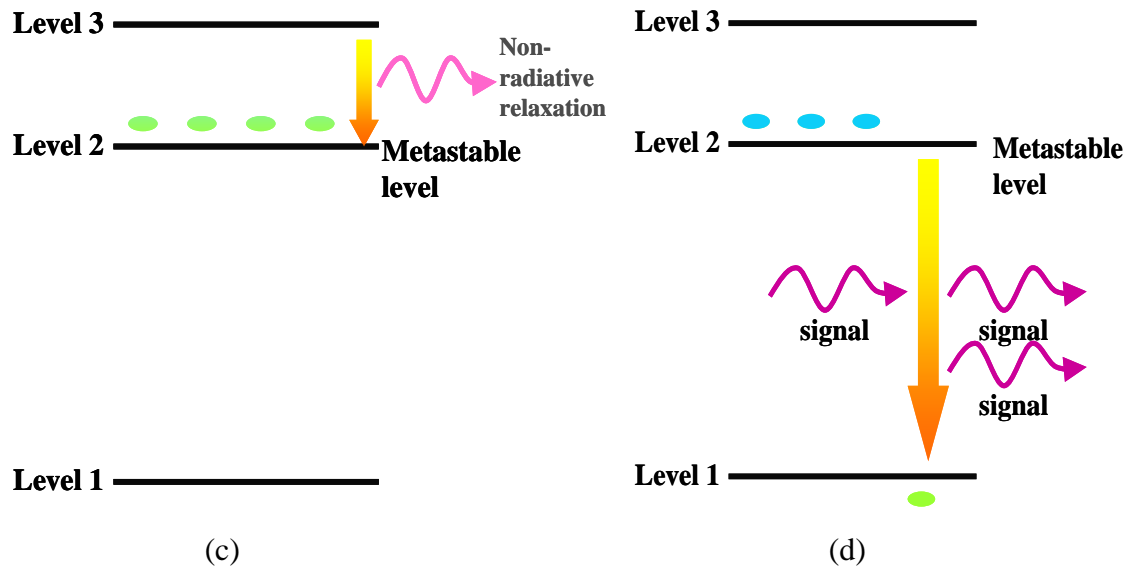


Figure 2.13 Three-level amplification system. (a) RE at rest, (b) pumping by 980nm light source, (c) non-radiative relaxation to metastable level, (d) stimulated emission.

Both systems resulted in more Er ions populated at the intermediate level. These ions tend to encountered transition from level 2 to level 1 by stimulation when an optical information signal appears near the inversely populated Er ions. The combination of stimulated transition with the stimulated emission of photons will resulted in input signal amplification [49].

2.3.3 THEORY OF ERBIUM AMPLIFICATION

The transition of two important energy levels (between $^4I_{13/2}$ level and $^4I_{15/2}$ level) of erbium incorporated into silica substrate naturally occur at a set of wavelengths around 1550 nm, where silica substrate exhibits minimum attenuation [50-54]. Such great coincidence has been the reason for the manifestation of Er-doped amplifier [49].

$\text{Er}^{3+} \rightarrow \text{Er}^{3+}$ energy transfer is an important dissipative mechanism in fiber amplification at 1500 nm [55]. Radiative energy transfer involves a photon emission by one ion and reabsorbed by another ion. Such process might cause emission spectrum distortion and radiative trapping that eventually leads to apparent artificial long excited-state lifetimes. This happens especially in highly concentrated or large volume samples which the ions are closely spaced.

The main process involved in between closely spaced ions is the excitation transfer without real photon exchange. In most situations, there is no significant amount of energy being transferred. However, the latter are rather similar to mechanisms encountered in the absorption and emission of real photons. The phonon-assisted process (absorption or emission of phonons) is dominated for crystals [56] and it is needed for energy conservation when the transition energies of ions are not equal or resonant.

The inefficiency for Er^{3+} devices at 1500 nm is believed to have cause by the energy transfer in between ions or more precisely cooperative up-conversion process (See Figure 2.14). In the up-conversion process, two excited ions are interacted and both are excited to the metastable ${}^4I_{13/2}$ level. Instead of emitting photon by stimulation, one of the ions (donor) can transfer all its energy to the other (acceptor) such that acceptor will be up-converted to ${}^4I_{9/2}$ state while leaving itself in ground state. The ${}^4I_{9/2}$ level will relax through multiphonon emission back to ${}^4I_{13/2}$ level. Thus, part of the energy absorbed by Er^{3+} will eventually encounter loss due to non-radiative relaxation in up-conversion process.

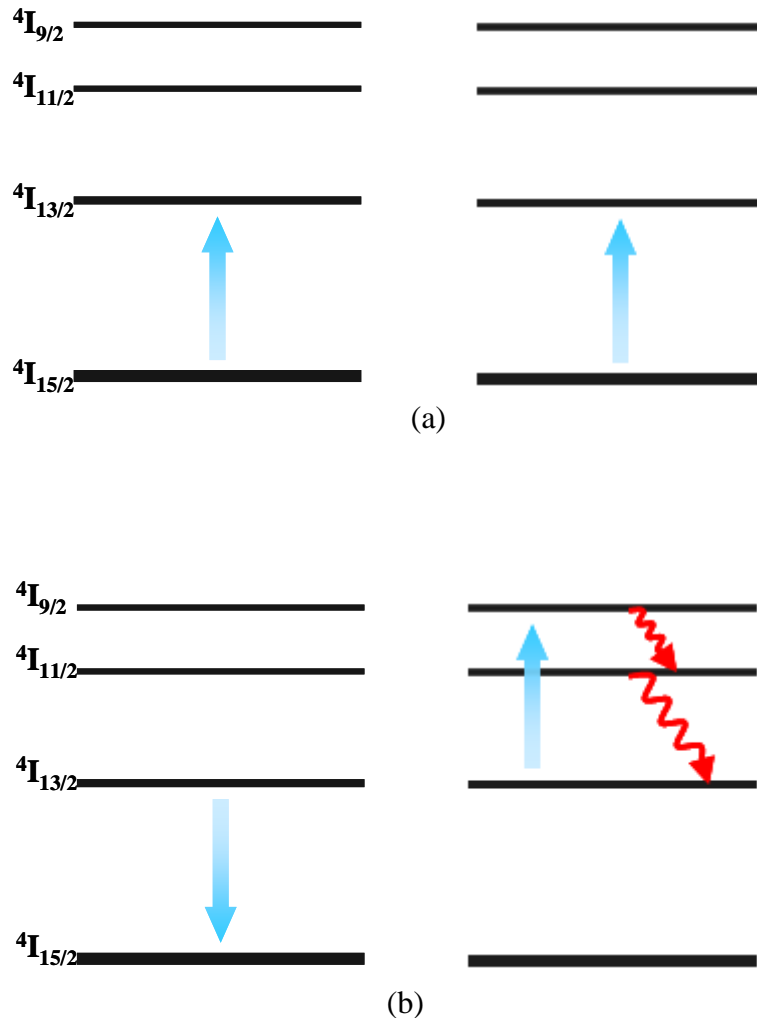


Figure 2.14 The up-conversion process illustrated for Er^{3+} . (a) both interacting ions are excited to the metastable $4I_{13/2}$ level, (b) the donor ion transfers all its energy to the acceptor, leaving itself in the ground state and the acceptor in the $4I_{13/2}$ state. For oxide glasses, the acceptor ion quickly decays nonradiatively back to the $4I_{13/2}$ level [23].

The performance of silica-based amplifier can be optimized by a suggested erbium concentration that is below 100 ppm [44]. However, indication shows Er concentration as high as 900 ppm with 14.4 dB gain has been reported [57].

High Er^{3+} concentration is necessary in short fiber or waveguide amplifiers [58-59]. Though, as stated, high concentration dopants in glass will result in few drawbacks such as signal quenching due to clustering. The incorporation of Yb^{3+} is an alternate solution as it allows impregnation of higher Er^{3+} concentrations and at the same time minimizes its quenching effect.

2.3.4 THEORY OF CO-DOPED AMPLIFICATION

In a typical energy transfer with two different species of ions, the ion that is optically excited is referred as the donor while the one that receives the excitation is known as the acceptor. The donor ion tends to absorb the photon and transfers its energy to a nearby acceptor. Another mechanism might occur if the donor concentration is high enough; the excitation might migrate among the strongly coupled donor ions. This is simplified as donor-donor transfer and it will proceed until an acceptor is found close enough to the excited donor and complete the donor-acceptor transfer process [23].

Yb offers a wide variety of pump wavelengths that allow full utilization of different high power sources in the range from 800 to 1100 nm [60-64]. When Yb³⁺ ions are introduced in the Er³⁺ system, Yb³⁺ ions tend to absorb most of the pump power and transfer the energy to the adjacent Er³⁺ ion [65-66]. Er³⁺ is excited by energy transfer from Yb³⁺ in order to increase the absorption cross section in a commonly 980 nm pumped glass system [67-68].

The multiple stage energy transfer process for the Yb³⁺/Er³⁺ co-doped system is illustrated in Figure 2.15. Initially, Yb³⁺ is excited to the ²F_{5/2} level from the ²F_{7/2} ground state. From there, standard radiative decay of Yb³⁺ back to the ground state tends to occur. Hence, the energy release will be absorbed by the adjacent Er³⁺. The ⁴I_{11/2} energy level for Er³⁺ might also encounter energy back transfer to Yb³⁺ ion (²F_{5/2}), but this possibility is relatively small. Therefore, most Er³⁺ ion is excited to the ⁴I_{11/2} state. Then, this ion tends to decay nonradiatively to the metastable level (⁴I_{13/2}) where population inversion occurs. Er³⁺ ion will fall to the ground state and emit new signal after stimulated with a pass-by signal.

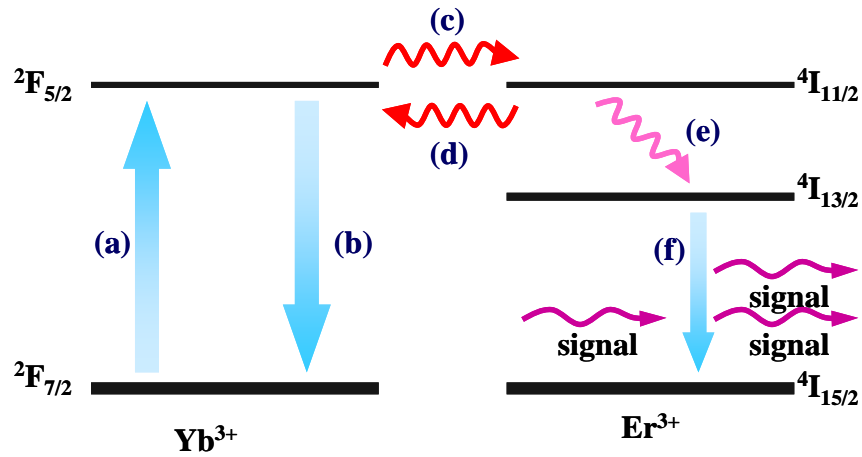


Figure 2.15 Energy transfer process for the Yb³⁺/Er³⁺ co-doped system. (a) excitation of Yb³⁺ ion, (b) standard radiative decay of Yb³⁺, (c) energy transfer (Yb³⁺→Er³⁺), (d) energy back transfers (Er³⁺→Yb³⁺), (e) Er³⁺ decay nonradiatively to metastable state, (f) emission by stimulation.

The effective silica-based Yb³⁺ sensitized Er³⁺ fiber was first fabricated in 1991 [69]. Yet, Yb³⁺ → Er³⁺ energy transfer have been used to improve the pumping efficiency of devices since the earliest days of solid-state lasers [23, 66] by reducing the energy transfer up-conversion between excited erbium ions [70]. In amplification, Yb-sensitized EDFAs have been demonstrated to provide higher and broader gain for a given pump level if compared to the conventional EDFAs [71].

REFERENCES:

- [1] Smith, F. Graham, King, Terry A., and Wilkins, Dan, "*Optics and Photonics: An Introduction*". 2nd ed. 2007. Chichester, England: John Wiley & Sons Ltd.
- [2] "*Introduction to glass integrated optics*".1992: Artech House.
- [3] Zachariassen, W. H., "The Atomic Arrangement In Glass." *J. Amer. Ceramic Soc.*, vol. 54 (10), (1932) p. 3841-3851.
- [4] Warren, B.E., Krutter, H., and Morningstar, O., "Fourier analysis of X-ray patterns of vitreous SiO₂ and B₂O₃." *Am. Ceram. Soc.*, vol. 19 (1936) p. 202-206.
- [5] Craig-Ryan, S.P. and Ainslie, B.J., "Glass Structure and Fabrication Techniques," in *Optical Fibre Lasers and Amplifiers*, France, Ed., ed Boca Raton, Florida, USA: CRC Press, Inc., 1991.
- [6] Varshneya, A. K., "*Fundamentals of inorganic glasses*".1994. San Diego: Academic Press Inc.
- [7] Tammela, S., Hotoleanu, M., Janka, K., Kiiveri, P., Rajala, M., Salomaa, A., Valkonen, H., and Stenius, P., "Potential of nanoparticle technologies for next generation erbium-doped fibers," in *Optical Fiber Communication Conference, 2004. OFC 2004*, 2004, p. 3 pp.
- [8] Gaskell, P.H., "The Structure of Amorphous Solids-A Perspective View." *J. Phys.*, vol. 46 (C8), (1985) p. 3.
- [9] Wang, J., Brocklesby, W. S., Lincoln, J. R., Townsend, J. E., and Payne, D. N., "Local structures of rare-earth ions in glasses: the 'crystal-chemistry' approach." *Journal of Non-Crystalline Solids*, vol. 163 (3), (1993) p. 261-267.
- [10] Warren, B.E., "Summary of work on atomic arrangement in glass." *Am. Ceram. Soc.*, vol. 24 (8), (1941) p. 256.

- [11] Huang, C. and Cormack, A. N., "*The Physics of Non-crystalline Solids*".1992. London: Taylor and Francis.
- [12] Doremus, R.H., "*Glass Science*".1973. New York: Wiley.
- [13] Watts, Samuel Pul, "Flame Hydrolysis Deposition of Photosensitive Silicate Layers Suitable for the Definition of Waveguiding Structures through Direct Ultraviolet Writing," PhD Thesis, Department of Electronics and Computer Science, University of Southampton, 2002.
- [14] Ainslie, B., Beales, K., Day, C., and Rush, J., "The design and fabrication of monomode optical fiber." *IEEE Journal of Quantum Electronics*, vol. 18 (4), (1982) p. 514-523.
- [15] Tien, T. Y. and Hummel, F. A., "The System SiO₂-P₂O₅." *Am. Ceram. Soc.*, vol. 45 (9), (1962) p. 422-424.
- [16] Ward, L., "*The optical constants of bulk materials and films*".1988. Bristol, London: Adam HilgerL IOP publishing Ltd.
- [17] "*Optical Fiber Telecommunications*".1979. New York: Academic Press.
- [18] Rawson, H., "*Properties and Applications of Glass: Glass Science and Technology*".1980, vol. 3. Amsterdam: Elsevier.
- [19] Li, Tingye, "*Optical fibre Communications: Fibre Fabrication*".1985, vol. 1. Orlando: Academic Press.
- [20] Tasker, G. W., French, W.G., Simpson, J.R., Kaiser, P., and Presby, H.M., "Low-loss Single-mode fibers with different B₂O₃-SiO₂ compositions." *Appl. Opt.*, vol. 17 (11), (1978) p. 1836-1842.
- [21] Koechner, Walter, "*Solid-State Laser Engineering*".1999. Berlin, Germany: Springer-Verlag.
- [22] Digonnet, M. J. F., "*Rare-earth doped fiber lasers and amplifiers*".2001: Marcel Dekker, Inc.

- [23] Miniscalco, William J., "Optical and Electronic Properties of Rare Earth Ions in Glasses," in *Rare-Earth-Doped Fiber Lasers and Amplifiers*, Digonnet, Ed., ed New York, USA: Marcel Dekker, Inc., 2001.
- [24] Guilhot, Dennis Alain "UV-written devices in rare-earth doped silica-on-silicon grown by FHD," PhD Thesis, Science and Mathematics, Optoelectronics Research Centre, University of Southampton, 2004.
- [25] Patek, K., "*Glass Lasers*".1970. London: ILIFFE Books, Butterworth.
- [26] Snitzer, E., "Recent Advances in Glass Laser," presented at the IEEE NEREM Massachusetts, USA, 1968.
- [27] Tang, F. Z., McNamara, P., Barton, G. W., and Ringer, S. P., "Multiple solution-doping in optical fibre fabrication II - Rare-earth and aluminium co-doping." *Journal of Non-Crystalline Solids*, vol. 354 (15-16), (2008) p. 1582-1590.
- [28] "*Glass Forming Systems: Glass Science and Technology*".1983, vol. 1. New York: Academic Press.
- [29] J. F. Macdowell, G. H. Beall, "Immiscibility and Crystallization in $\text{Al}_2\text{O}_3\text{SiO}_2$ Glasses." *Journal of the American Ceramic Society*, vol. 52 (1), (1969) p. 17-25.
- [30] Dhar, A., Pal, A., Paul, M. C., Ray, P., Maiti, H. S., and Sen, R., "The mechanism of rare earth incorporation in solution doping process." *Opt. Express* vol. 16 (2008) p. 12835-12846
- [31] Ainslie, B. J., Craig, S. P., Davey, S. T., and Wakefield, B., "The fabrication, assessment and optical properties of high-concentration Nd^{3+} - and Er^{3+} -doped silica-based fibres." *Materials Letters*, vol. 6 (5-6), (1988) p. 139-144.
- [32] Simpson, J. R. and Macchesney, J. B., "Optical fibres with an Al_2O_3 -doped silicate core composition." *Electronics Letters*, vol. 19 (7), (1983) p. 261-262.

- [33] Laming, R. I., Townsend, J. E., Payne, D. N., Meli, F., Grasso, G., and Tarbox, E. J., "High-power erbium-doped-fiber amplifiers operating in the saturated regime." *IEEE Photonics Technology Letters*, vol. 3 (3), (1991) p. 253-255.
- [34] Massicott, J. F., Wyatt, R., Ainslie, B. J., and Craig-Ryan, S. P., "Efficient, high power, high gain Er^{3+} doped silica fibre amplifier," in *Proc. SPIE*, 1991, p. 93-102.
- [35] Kagi, N., Oyobe, A., and Nakamura, K., "Efficient optical amplifier using a low-concentration erbium-doped fiber." *IEEE Journal of Quantum Electronics*, vol. 2 (8), (1990) p. 559-561.
- [36] Ainslie, B.J., Craig, S.P., Davey, S.T., Barber, D.J., Taylor, J.R., and A. S, L. Gomes, "Optical and structural investigation of Nd^{3+} in silica-based fibers." *Mater. Sci.*, vol. 6 (1987) p. 1361-1363.
- [37] Stone, J. and Burrus, C.A., "Nd-doped SiO_2 Lasers in end pumped fibre geometry." *Appl. Phys. Lett.*, vol. 23 (1973) p. 388-389.
- [38] MacChesney, J. B. and Simpson, J.R., "Optical waveguides with novel compositions," in *Proc. OGC'85*, 1985, p. 100.
- [39] Arai, K., Namikawa, H., Kumata, K., Honda, T., Ishii, Y., and Handa, T., "Aluminium or phosphorus co-doping effects on the fluorescence and structural properties of neodymium-doped silica glass." *Appl. Phys.*, vol. 59 (1986) p. 3430-3436.
- [40] Poole, S. B., "Fabrication of Al_2O_3 co-doped optical fibres by a solution-doping technique," in *Optical Communication, 1988. ECOC 88. Fourteenth European Conference on (Conf. Publ. No.292)*, 1988, p. 433-436
- [41] Ainslie, B. J., Craig, S. P., and Davey, S.T., "The fabrication and optical properties of Nd^{3+} in silica-based optical fibers." *Materials Letters*, vol. 5 (1987) p. 143-146.

- [42] Tang, F. Z., McNamara, P., Barton, G. W., and Ringer, S. P., "Multiple solution-doping in optical fibre fabrication I - Aluminium doping." *Journal of Non-Crystalline Solids*, vol. 354 (10-11), (2008) p. 927-937.
- [43] Namikawa, H., Kazuo, A., K.Kumata, Ishii, T., and Tanaka, H., "Preparation of Nd-doped SiO₂ glass by plasma torch CVD." *Appl. Phys.*, vol. 21 (1982) p. L360-L362.
- [44] Shimizu, M., Yamada, M., Horiguchi, M., and Sugita, E., "Concentration effect on optical amplification characteristics of Er-doped silica single-mode fibers." *IEEE Photonics Technology Letters*, vol. 2 (1), (1990) p. 43-45.
- [45] Simpson, J. R., Shang, H. T., Mollenauer, L. F., Olsson, N. A., Becker, P. C., Kranz, K. S., Lemaire, P. J., and Neubelt, M. J., "Performance of a distributed erbium-doped dispersion-shifted amplifier." *IEE/OSA Lightwave Technol.*, vol. LT-9 (1991) p. 228-233.
- [46] R.Simpson, Jay, "Rare Earth Doped Fiber Fabrication: Techniques and Physical Properties," in *Rare-earth-doped Fiber Lasers and Amplifiers*, Digonnet, Ed., 2 ed New York, USA: Marcel Dekker, Inc, 2001.
- [47] Izumitani, T.S., "*Optical Glass*".1986. New York: American Institute of Physics.
- [48] Yamshita, T., Amano, S., I. Masuda, Izumitani, T., and Ikushima, A., "Nd and Er doped phosphate glass fiber lasers," in *CLEO'88*, 1988.
- [49] Mynbaev, Djafar K. and Scheiner, Lowell L., "*Fiber-optic Communications Technology*".2001. Upper Saddle River, New Jersey: Prentice-Hall, Inc.
- [50] Hoven, G. N. van den, Koper, R. J. I. M., Polman, A., Dam, C. van, Uffelen, J. W. M. van, and Smit, M. K., "Net optical gain at 1.53 μm in Er-doped Al₂O₃ waveguides on silicon." *Appl. Phys. Lett.*, vol. 68 (1996) p. 1886.

- [51] Kenyon, A. J., "Recent developments in rare-earth doped materials for optoelectronics." *Progress in Quantum Electronics*, vol. 26 (4-5), (2002) p. 225-284.
- [52] Li, C. R., Song, C. L., Li, S. F., and Rao, W. X., "Deposition of Er:Al₂O₃ films and photoluminescence characteristics." *Chinese Physics Letters*, vol. 20 (2003) p. 1613.
- [53] Yang, K.S., Liang, H.L., Cheng, G., and Meng, J., "Investigation on preparation and fluorescence properties of oxy-fluoride glass co-doped with Er³⁺ and Yb³⁺." *Rare Earths*, vol. 22 (2004) p. 458.
- [54] Li, Chengren, Lei, Mingkai, Li, Shufeng, Liu, Yufeng, and Song, Changlie, "Fabrication and photoluminescence characteristics of nonuniform Yb-Er codoped films." *Journal of Rare Earths*, vol. 26 (1), (2008) p. 31-34.
- [55] Wyatt, R., "Spectroscopy of rare earth doped fibres," in *Proc. SPIE*, 1989, p. 54-64.
- [56] Strauss, E., Miniscalco, W. J., Hegarty, J., and Yen, W. M., "Investigation of resonant energy transfer for LaF₃:Pr³⁺." *Phys.*, vol. C 14 (1981) p. 2229-2236.
- [57] Suyama, M., Nakamura, K., and S.Kashiwa, "14.4-dB gain of erbium-doped fiber amplifier pumped by 1.49 μm laser diode.," in *Proc. OFC'89*, 1989.
- [58] Nilsson, J., Scheer, P., and Jaskorzynska, B., "Modeling and optimization of short Yb³⁺-sensitized Er³⁺-doped fiber amplifiers." *IEEE Photonics Technology Letters*, vol. 6 (3), (1994) p. 383-385.
- [59] Lumholt, O., Rasmussen, T., and Bjarklev, A., "Modelling of extremely high concentration erbium-doped silica waveguides." *Electronics Letters*, vol. 29 (5), (1993) p. 495-496.
- [60] Minelly, J. D., Barnes, W. L., Laming, R. I., Morkel, P. R., Townsend, J. E., Grubb, S. G., and Payne, D. N., "Diode-array pumping of Er³⁺/Yb³⁺ Co-doped

- fiber lasers and amplifiers." *IEEE Photonics Technology Letters*, vol. 5 (3), (1993) p. 301-303.
- [61] Paschotta, R., Nilsson, J., Barber, P. R., Caplen, J. E., Tropper, A. C., and Hanna, D. C., "Lifetime quenching in Yb-doped fibres." *Optics Communications*, vol. 136 (5-6), (1997) p. 375-378.
- [62] Weber, M. J., Lynch, J. E., Blackburn, D. H., and Cronin, D. J., "Dependence of the stimulated emission cross section of Yb³⁺ on host glass composition." *IEEE Journal of Quantum Electronics*, vol. QE-19 (1983) p. 1600-1608.
- [63] Zou, X. and Toratani, H., "Evaluation of spectroscopic properties of Yb³⁺-doped glasses." *Phys. Rev. B*, vol. 52 (22), (1995) p. 15889-15897.
- [64] Takabe, H., Murata, T., and Morinaga, K., "Composition dependence of absorption and fluorescence of Yb³⁺ in oxide glasses." *J. Amer. Ceramic. Soc.*, vol. 79 (3), (1996) p. 681-687.
- [65] Achtenhagen, M., Beeson, R. J., Pan, F., Nyman, B. A. Nyman B., and Hardy, A. A. Hardy A., "Gain and noise in ytterbium-sensitized erbium-doped fiber amplifiers: measurements and simulations." *Journal of Lightwave Technology*, vol. 19 (10), (2001) p. 1521-1526.
- [66] Snitzer, E. and Woodcock, R., "Yb³⁺-Er³⁺ glass laser." *Appl. Phys. Lett.*, vol. 6 (1965) p. 45-46.
- [67] Townsend, J. E., "The development of optical fibres doped with rare-earth ions," PhD Thesis, Electronics and Computer Science, University of Southampton, 1990.
- [68] Funk, D. S., Veasey, D. L., Peters, P. M., Sanford, N. A., and Fontaine, N. H., "Erbium/ytterbium-codoped glass waveguide laser producing 170 mW of output power at 1540 nm," in *Proc. Opt. Fiber Commun.*, 1999, p. 32-34.

- [69] Townsend, J. E., Barnes, W. L., Jedrzejewski, K. P., and Grubb, S. G., "Yb³⁺ sensitized Er³⁺ doped silica optical fiber with ultra high efficiency and gain." *Electronics Letters*, vol. 27 (21), (1991) p. 1958-1959.
- [70] Vienne, G. G., Caplen, J. E., Liang, Dong, Minelly, J. D. A. Minelly J. D., Nilsson, J. A. Nilsson J., and Payne, D. N. A. Payne D. N., "Fabrication and characterization of Yb³⁺:Er³⁺ phosphosilicate fibers for lasers." *Journal of Lightwave Technology*, vol. 16 (11), (1998) p. 1990-2001.
- [71] Namkyoo, Park, Wysocki, P., Pedrazzani, R., Grubb, S., DiGiovanni, D., and Walker, K., "High-power Er-Yb-doped fiber amplifier with multichannel gain flatness within 0.2 dB over 14 nm." *IEEE Photonics Technology Letters*, vol. 8 (9), (1996) p. 1148-1150.

CHAPTER 3

PRINCIPLES AND METHODS OF FABRICATION

Different methods have been implemented for fabrication of rare-earth doped waveguide amplifiers. These include thermal and field-assisted ion exchange in bulk-doped phosphate and silicate glasses [1-5]. For several rare-earth doped dielectric films for optical channel waveguides, film deposition such as radio frequency sputtering [6-7], plasma-enhanced chemical vapor deposition [8], flame hydrolysis [9], ion implantation [10], laser ablation [11] and sol-gel deposition [12-13] has been commonly used. In this dissertation, glass films deposition is restricted to the flame hydrolysis method.

There are two main techniques for doping flame hydrolysis deposition (FHD) glass layer with rare-earth. These are solution doping and aerosol doping. Basically, solution doping technique has been developed for fiber manufacture and it was first used for rare-earth doping in 1973 by Stone and Burrus [14]. This technique apply the similar concept for the deposited FHD layer that involves doping a robust soot layer that is partially sintered [15]. This is done by immersing the soot layer in a solution with the RE solutes [16-18]. Then, the sample is dried and consolidated into a solid glass layer. The concentration that retained in the soot layer greatly relies on the solution concentration, immersion period and the pre-sintering temperature of the soot layer [19].

The experimental investigations described in this dissertation were conducted exclusively in rare-earth doped into partially sintered soot layer and then followed by consolidation of glass layer. Each of the samples from either group was characterized using EDX, and prism coupler machine was used for full sintered glass. This chapter presents details of the procedures used to fabricate the rare-earth doped samples and the principles involved beneath the fabrication process.

3.1 PLANAR GLASS SAMPLES

The scope of this dissertation is limited to silica-on-silicon substrate. Silicon wafers are good substrate for fabricating a high quality film layers because they are very flat, smooth and available in large sizes. Meanwhile, silica is the common material found in the existing silica optical fibers network. Its refractive index is identical to the fibers and this ensures a low optical loss when planar and fiber systems are connected. This is the reason that make silica-on-silicon a favored technology. Glass layer can be fabricated layer by layer via flame hydrolysis deposition technique.

3.1.1 FLAME HYDROLYSIS DEPOSITION (FHD)

Planar films made by Flame Hydrolysis Deposition was first reported in 1983 [20]. FHD is reliable silica-based optical waveguide technology as it fabricates a fiber compatible low-loss integrated optical devices [21]. FHD also deposit optical quality and thick cladding layers such that the channel waveguides are completely embedded. Besides, this technology is capable of synthesise core glasses having the same refractive index but different minimum sintering temperatures by varying the concentration levels of the silica dopants [22]. Low loss films as low as 0.01dB/cm has been produced by FHD [21].

Compared to PECVD processes, the layers produced by FHD can be uniform, easier to prevent foreign particles contamination and contained lack of large cluster complexes formation [23]. Most importantly, FHD is well adaptable to solution doping process. Rare-earth doped FHD produced layers have been successfully demonstrated [9, 24-26]. The typical fabrication stages of RE-doped silica-based waveguide are shown in Figure 3.1.

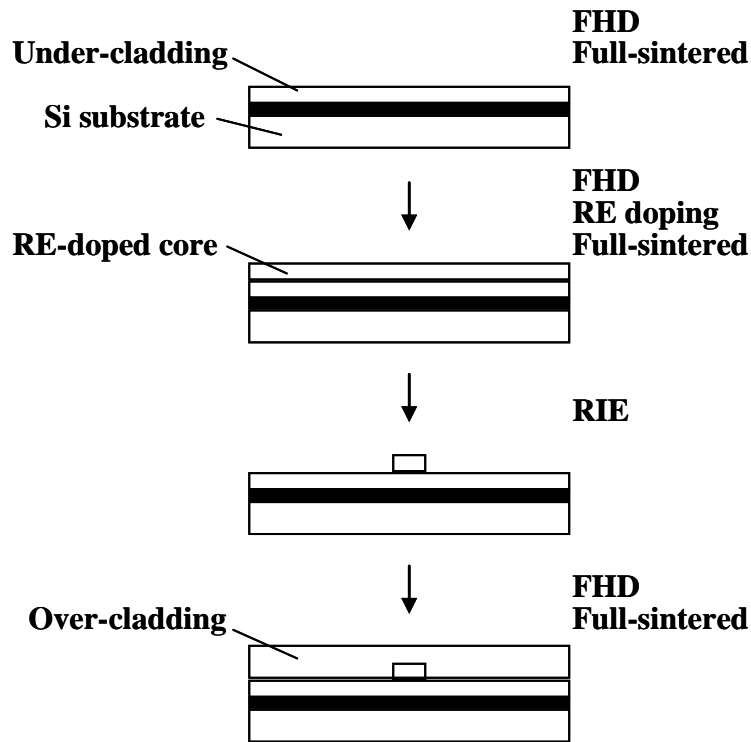


Figure 3.1 Fabrication stages of RE-doped silica-based waveguide [18].

Generally, silica films are synthesized by flame hydrolysis reaction in the oxy-hydrogen torch. This technique implements an oxy-hydrogen combustion method where reagents are flowed in the flame and being oxidized. The reagents used are liquid halide materials such as silicon tetrachloride (SiCl_4), phosphorous oxytrichloride (POCl_3) and germanium tetrachloride (GeCl_4), which are all vaporized in a halide container (bubblers) (Figure 3.2). Helium is used as the carrier gas to transport the vapour into flame. The quantity of halide transported to the burner is controlled by adjusting the temperature of the bubbler and flow rate of the gas through the bubbler. Three mass flow controllers (MFC) are responsible in monitoring the flow rate of each individual gas supply.

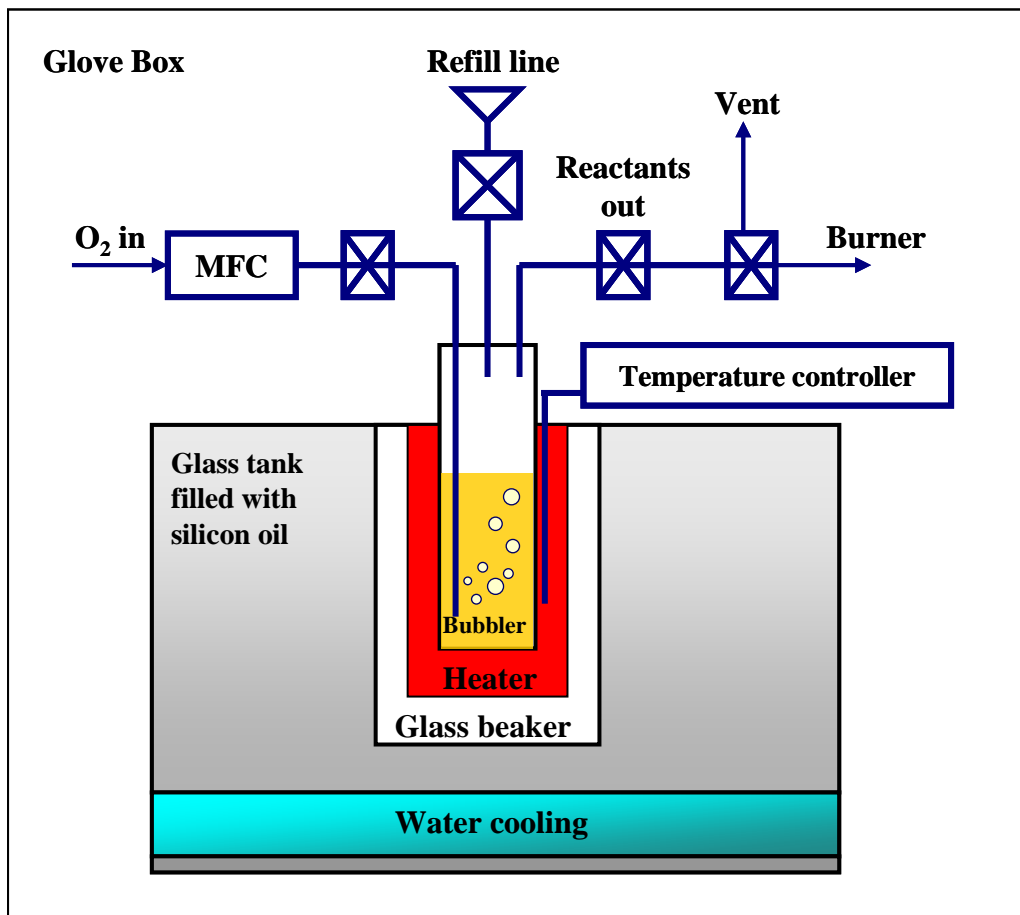


Figure 3.2 Gas supply system for FHD [23].

Meanwhile, BCl_3 at ambient temperature is in a high vapour pressure and this allows it to be treated as gas. Unlike other halides, BCl_3 is independent to carrier gas and it is flow from a cylinder into the pipe work through a series of valves. The flow rate of BCl_3 is regulated via an MFC before entering the burner. Once all the gases are mixed together in the flame, fine oxide particles (soot particle) are formed and deposited on the substrate.

During the deposition process, the flame is translated across the substrate to deposit uniform layers of soot (Figure 3.3). Different thickness of silica layer can be obtained by controlling the quantity of soot deposited. This is done by varying the speed of the translation stage (turntable), the gas flow rate and number of process passes. Next, the low-density soot layer is then consolidated through exposure to high temperatures

(~1350 °C) in a furnace to form a transparent fully dense glass layer. A partially consolidated porous soot layer is required for RE incorporation. Therefore, the soot layer is half sintered at 850 °C. This will be elaborated in the next section.

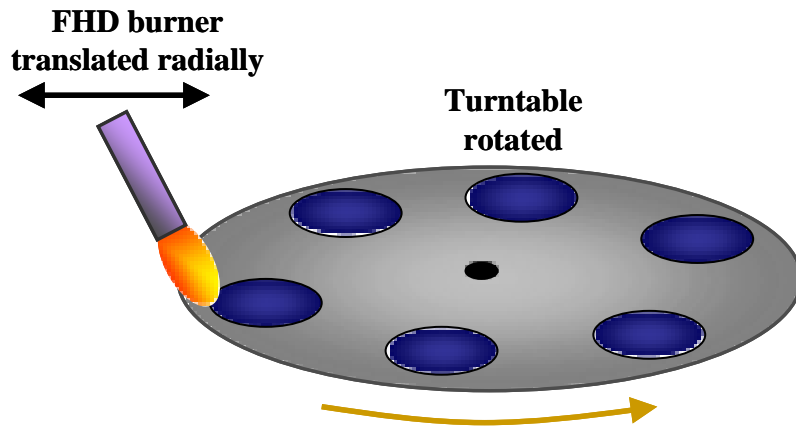


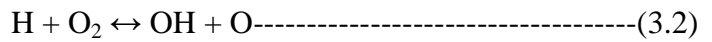
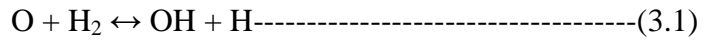
Figure 3.3 Schematic of typical Flame Hydrolysis Deposition process.

The overall system is computerized with a program to control the MFC, control valves and temperature controller devices, and record the data for each deposition. Besides, the information for real time monitoring of the deposition is displayed. With this program, user is allowed to select the required layer recipe, monitor the deposition process and do purging when the deposition is done. The purpose of purging is to clean and clear the entire chemical residue trap within the chemical pipe line and it is usually applies using nitrogen. It is recommended to pursue purging at least for 2 hours whenever FHD process is being carried out. In this dissertation, recipe “core 26” with five deposition passes has been used to prepare the core layer for doping.

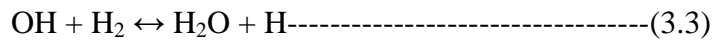
Table 3.1 Recipe “Core 26”.

Reagents	Composition (sccm)
SiCl ₄	50
GeCl ₄	40
POCl ₃	35
BCl ₃	30

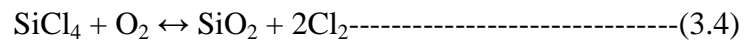
The reagents used are silicon, germanium, phosphorus and boron liquid halides. As mentioned earlier, these reagents are injected into the highly reactive environment of oxy-hydrogen flame. Below are the endothermic reactions for an oxygen-hydrogen flame which lead to chain branching:



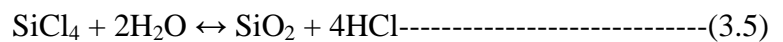
As a result, an excess population of free atoms and radicals are build up in the reaction zone [23, 27]. The following are the propagation step:



Oxidation occurs at the centre of the flame (approximately 2000 °C) where silica particles are formed by direct oxidation. The oxidation can be described by the reaction below:



Meanwhile, hydrolysis occurred at the temperatures under 1200 °C. HCl are formed as Cl₂ reacts with water.



SiO₂, B₂O₃ and P₂O₅ particles are all formed within the flame, while GeO₂ can be formed within the flame and also condense on the substrate [28].

Generally, FHD process is a reliable and flexible method for producing the structure of planar waveguide. By adjusting the composition of the dopants,

germanium-boron-phosphorus doped silica layers allowed us to reduce the sintering temperature from 1400°C to a lower one ranged between 1000 to 1400 °C. This is important as silicon wafers tend to melt at 1410 °C [23].

FHD system (FRS 300 from Semitel) consists of its own dedicated scrubbing system posited near to the FHD rig. Scrubber unit operates at below atmospheric pressure in order to increase the extraction rate happened within the FHD rig. The scrubbing performed using liquid of sodium hydroxide with water to remove hazardous HCl.

3.1.2 SINTERING

Sintering occurs when silica soot deposited by FHD is heated to near its melting point and fully densified into glass. This involved in heat treatment of powder compact at an elevated temperature and normally diffusional mass transport occurs. Heating encourages sufficient degree of particle softening and resulting surface tension pulling particle together. Surface area tends to decrease and brought to a decrease in free energy as well. Such process is irreversible [29]. The mechanism involves for such sintering of soot is known as viscous sintering [30]. During the sintering process, the centre-to-centre separation between adjacent particles will be reduced [23, 31]. This will eventually leads to necking of particles until the silica particles joined together and pores are closed to form network with a random connected bridges [32]. In this experiment, full sinter process is performed after RE impregnation via solution doping.

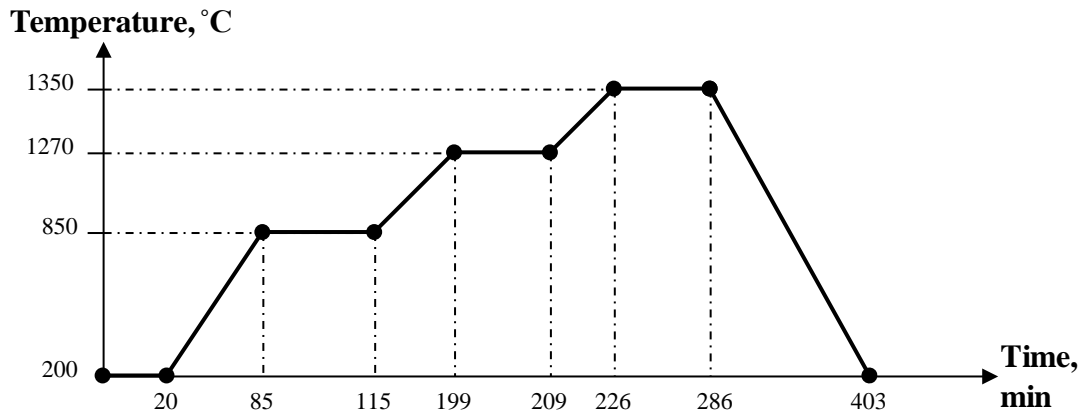


Figure 3.4 Diagram showing the temperature and time parameters for full-sintering of underclad/core.

To form a porous silica film, silica soot has to be heated below its melting point such that it is partially sintered where pores are still available. Sintering temperature is a key parameter in controlling the pore size for incorporation of dopant via solution doping. More precisely, pre-sintering temperature process takes control over the porosity and density as well as the pore size distribution. All of these criteria can either facilitate or hamper the rare-earth impregnation into glass matrix [33]. Various pre-sintering temperature (500 to 900 °C) has been prepared to investigate the optimum pre-sintering temperature for proper solution doping.

The soot layer deposited from the FHD system is moved into the furnace (HVH 410 from Hanvac) for pre-sintering such that a partially sintered medium is prepared for incorporation of additional RE dopant via solution doping. The pre-sintered temperature is 850 °C ramping up from 200 °C with a heating ramp rate of 5 °C/min. The pre-sintered temperature is held for approximately 45 minutes before it was ramping down to 200 °C with a heating ramp rate of 15 °C/min. The overall pre-sintering process is carried out under oxygen (2 sccm) and helium (2 sccm) flow conditions.

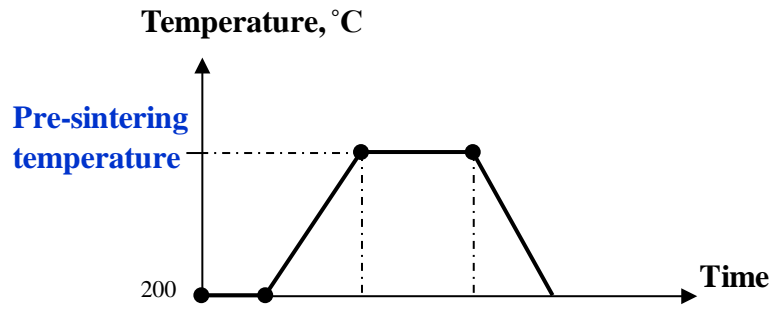


Figure 3.5 Diagram showing temperature and time control for half-sintering of soot layer.

3.2 SOLUTION DOPING

3.2.1 PRINCIPLES OF SOLUTION DOPING

The principle of solution doping involves immersing any porous silica based material into a rare-earth salt liquid solution [34]. According to a few publications, the porous silica acts as a sponge, taking up the solution. Precisely, the mechanism of rare-earth incorporation in porous silica involved capillary action and chemical absorption [23, 35-36]. Therefore, the porosity of the silica layer which is controlled by the pre-sintered temperature takes an important role to ensure a sufficient concentration of rare-earth impregnation [33, 37-38]. Besides, solution concentration and immersion period are also important in facilitate rare-earth impregnation into the porous silica [19]. The above matter is crucial in order to achieve efficient rare-earth retention in silica layer.

3.2.2 SOLVENT

The selectivity of solvent for solution doping must fulfil few conditions. Firstly, the solvent must be a material in which the half-sintered soot insoluble. Then, the dopant must be highly and completely soluble in the selected solvent. Finally, it has to be ensured that no residue is left after soaking and dehydration. For the typical soot

which contained germania or phosphoria, liquids such as water, HCl and other organics are appropriate solvents [39], but the two main contenders are water and simple alcohols (eg. ethanol). Some of the reasons that bring to such selection are because both solvents are readily available in high purity form and are safe to handle.

3.2.2.1 WATER

The combination of solution-doping technique with MCVD has been reported [19] where an unsintered (porous) silica layer is deposited inside the silica tube by MCVD process before the tube is soaked in an aqueous rare-earth chloride solution for about 1 hour. Then the solution is drained follow by drying the impregnated layer at high temperature in a chlorine/oxygen gas flow environment. Al have been incorporated such method as well [40] and doped fibers with background losses of 0.3 dB km^{-1} has been produced [41-42].

However, the existence of OH^- ions tend to bring out a major absorption band about 1390 nm which will eventually increase the fiber losses. The magnitude of the OH^- impact is estimated to have contributed to an excess loss of 48 dB/km at 1385 nm by one part in 10^6 . Hence, it is no doubt that the presence of OH^- ions with just few hundred ppm will place a significant affection on the performance of laser ions. This happens because OH^- ions tend to form phonon interaction with rare-earth ions and result in multiphonon non-radiative relaxation (quenching) [43-44]. However, this quenching effect can be brought to minimum level as long as the OH^- ions are effectively and rapidly removed. Fibers containing less than 40 ppb have been successfully prepared by VAD technique by a simple drying technique [45-46].

3.2.2.2 ALCOHOL

In an attempt to avoid OH^- ion contamination, alcohol solution such as ethanol is another solvent that has been used with rare-earth salts for solution doping process [14, 47-50]. Alcohol is less polarized, so, it is less likely to form bonding with the glass network. On the other hand, alcohol liquid is more volatile than water; this means that it can be easily evaporated. Besides, the complexes that form in alcohol solution are much larger than the hydrated ions in aqueous solution [51]. Therefore, steric hinderance occurred and become significant. This is because of the physically large complex tends to prevent other ions from being absorbed into the porous soot. For worse, diffusion of ion through the soot surface might be prohibited. Such poor diffusion will eventually leads to a greater possibility of clustering [52] since the dopant ions tend to agglomerate in a limited accessible sites.

Besides that, there is another drawback to the use of alcohols; the solubility of some high purity materials (eg. $\text{AlCl}_3 \cdot 6\text{H}_2\text{O}$) in ethanol are relatively low. Plus, such highly concentrated alcoholic solutions have a much higher viscosity if compare to the aqueous solution. Again, these two drawbacks will cause slow reagent diffusion through the soot and the penetration is only limited to low porosity soot. Therefore, the selection of appropriate solution's viscosity for different porous soot layer morphology is an important criteria [53].

It has been reported that in order to produce a glass with a given refractive index, higher concentration is needed in alcoholic solution compare to aqueous solutions [54]. Alcoholic solutions are preferred as an alternative for the OH^- effect since removal of dehydration can be achieved more easily. However, the combination of low solubility of the precursors, high viscosity solutions and more complicated solution chemistry will potentially limit the effectiveness of ions incorporation. Further more, the absolute

concentration of dopant, control of ion concentration and distribution of dopant over the glass could be reduced.

A pure silica soot boule with a porosity of 60-90 % (pore diameter of 0.001-10 μm) fabricated by flame hydrolysis was immersed in a dopant-salt methanol solution for 1 hour and dried for 24 hours followed by sintering in a $\text{He}/\text{O}_2/\text{Cl}_2$ atmosphere for bubble-free glass rod formation. The dopant concentration can be controlled by varying the ion concentration in the solution. This technique is applied in the incorporation of Nd and Ca in silica which is more referred as molecular stuffing [55-56].

All sorts of alcohol such as ethyl alcohol, ethyl ether and acetone have been used for Al and rare-earth halides. The replacement of non-aqueous solvents has produced doped fiber with a relatively low OH impurity level; contained less than 10 dB m^{-1} absorption at 1.38 μm [57]. Though, it is also possible to produce low OH fibers via aqueous solution doping as long as dehydration technique is done properly. Hence, water has been used as the solvent throughout the whole experiment.

3.2.3 SOLUTE

Rare-earth ion halide precursors are readily available in high purity form, solid at room temperature, quite safe to be handled and most importantly soluble in water; this makes it a suitable solute to be used in solution doping process [39]. The chemistry of the rare-earth ion chlorides in aqueous solution is simple [51]; cations are hydrated and formed $\text{RCl}_{3-x}(\text{H}_2\text{O})_n^{x+}$, where R is a rare-earth ion and n and x are integers ($0 < x < 3$, typically $n=6$). Though, water is normally found complexed at high purity of rare-earth compounds. There are two impurities involved; water, which is present with rare-earth salts and chlorides. Water is an ultimate solvent and has been used through this

dissertation. Although it has limitations, but the issues occurred are well known and can be easily overcome.

According to Townsend, charge distribution is likely to have altered the effectiveness of dopant adsorption where cationic rare-earth ions tend to accumulate and bond at the more negative charged point in an oxygen rich system. Rare-earth ions are predicted and proven to be more soluble in P_2O_5 or Al_2O_3 doped glass matrix than in silica or germanosilicate structure and hence, a higher incorporation for unit solution strength has been approached.

3.2.4 METHODOLOGY

Two groups of co-dopant are used: Er/Al and Er/Yb. Two type of aqueous-based solutions were prepared using high purity $ErCl_3 \cdot 6H_2O$ (99.9% purity, Aldrich), $AlCl_3 \cdot 6H_2O$ (99.9% purity, Fluka) and $YbCl_3 \cdot 6H_2O$ (99.9%, Aldrich). The first contained erbium and aluminium with either keeping erbium at a fixed concentration (0.02 and 0.04 M) and varying aluminium concentration or vice versa, keeping aluminium at a fixed concentration (0.4 M) and varying erbium concentration. The second contained erbium and ytterbium with a fixed erbium concentration of 0.02 M and varying ytterbium concentration; ytterbium was also fixed at 0.02 M while varying erbium concentration. The solution strength used for both type of co-doping is shown in Table 3.2.

Table 3.2 Solution strength for co-doping

Experiment	Al concentration (M)	Er concentration (M)	Yb concentration (M)
1	0.05, 0.1, 0.2, 0.3, 0.4	0.02 (fixed)	
2	0.1, 0.2, 0.4, 0.6, 0.8	0.04 (fixed)	
3	0.4 (fixed)	0.01, 0.02, 0.04, 0.05, 0.06	
4		0.02 (fixed)	0.02, 0.03, 0.04, 0.05, 0.06
5		0.02, 0.03, 0.04, 0.05, 0.06	0.02 (fixed)

The solution for solution doping was prepared in different concentrations (as indicated in Table 3.2) by dissolving $\text{ErCl}_3 \cdot 6\text{H}_2\text{O}$ with $\text{AlCl}_3 \cdot 6\text{H}_2\text{O}$ or $\text{YbCl}_3 \cdot 6\text{H}_2\text{O}$ powder in 100 ml deionised (DI) water. The porous soot layer which has been prepared earlier was soaked in aqueous-based solution for one hour (refer Figure 3.6). Then, the soaked layer was taken out and dried in the room temperature for ~16 hours followed by heating in the oven at ~100C for 10 minutes to 3 hours. Silica gel as moisture-absorbent was placed in the oven to ensure the inner atmosphere of oven was free from excessive moisture. The samples of the soaked/dried soot layers were carefully diced into two; one of them was full sintered into a dense silica glass film by heat treatment at 1320~1350 °C.

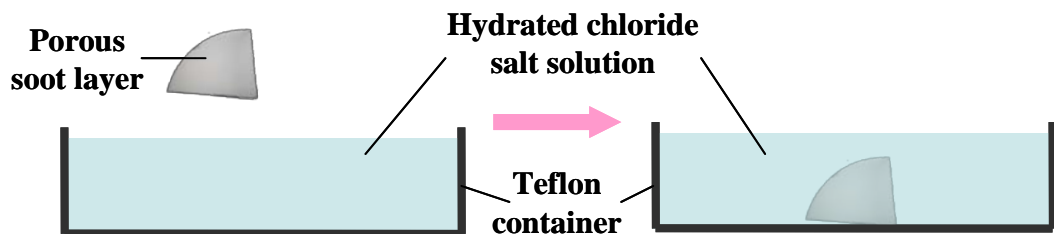


Figure 3.6 Schematic showing the solution doping process of a quarter wafer.

Besides varying the solution concentration, few immersion periods were used for solution doping of Er/Yb at a concentration of 0.02 M, ratio 1:1. The porous soot layers were soaked in the solution with the immersion period of 10 seconds, 15 minutes, 1 hour and ~16 hours. Drying process was pursued as previous procedure. Each sample was divided into half such that half of it was fully sintered.

Above were the typical method for solution doping. Apart from that, multiple cycles of solution doping has been implemented. After solution soaking and drying, the doped soot layer was heated in the furnace at 800 °C for 15 min. Using the identical deposited soot layer, the doped soot layers were prepared with one, two and three cycles of soaking in the Er/Yb (0.02/0.02 M) solution followed by drying at room temperature for ~16 hours and heating up in the oven (~100 °C) for about 10 minutes to 3 hours.

Before the next cycle was applied, the soaked soot layer has to be heated in the furnace at 800 °C. This step is crucial as this converts the soluble hydrated chloride salts within the porous soot layer into insoluble oxides. It is believed that by such heating step, the precursor used tends to be trapped within the soot and preventing it from loss due to dissolution during subsequent cycles [35, 58]. After the whole cycle was completed, again, half part of each of the sample was full sintered into dense glass.

Characteristic of both the porous and fully dense doped glass layer were investigated. The microstructure and morphology of the porous doped soot layers were examined through scanning electron microscope (SEM, LEICA S440). The dopants retention within soot layer was determined by energy dispersive spectrometry (EDX, HP Vectra XM Series 3 5/120 from Hewlett Packard). The thickness and refractive index of the co-doped silica films were measured by prism coupler (SAERON SPA 4000) at a wavelength of 1550 nm.

REFERENCES:

- [1] Saruwatari, Masatoshi and Izawa, Tatsuo, "Nd-glass laser with three-dimensional optical waveguide." *Appl. Phys. Lett.*, vol. 24 (1974) p. 603.
- [2] Malone, K. J., Sanford, N. A., and Hayden, J. S., "Integrated optic laser emitting at 906, 1057, and 1358 nm." *Electronics Letters*, vol. 29 (8), (1993) p. 691-693.
- [3] Feuchter, T., Mwarania, E. K., Wang, J., Reekie, L., and Wilkinson, J. S., "Erbium-doped ion-exchanged waveguide lasers in BK-7 glass." *IEEE Photonics Technology Letters*, vol. 4 (6), (1992) p. 542-544.
- [4] Vossler, G. L., Brooks, C. J., and Winik, K. A., "Planar Er:Yb glass ion exchanged waveguide laser." *Electronics Letters*, vol. 31 (14), (1995) p. 1162-1163.
- [5] Fournier, P., Meshkinfam, P., Fardad, M. A., Andrews, M. P., and Najafi, S. I., "Potassium ion-exchanged Er-Yb doped phosphate glass amplifier." *Electronics Letters*, vol. 33 (4), (1997) p. 293-295.
- [6] Yan, Y. C., Faber, A. J., Waal, H. de, Kik, P. G., and Polman, A., "Erbium-doped phosphate glass waveguide on silicon with 4.1 dB/cm gain at 1.535 μm ." *Appl. Phys. Lett.*, vol. 71 (1997) p. 2922.
- [7] Shmulovich, J., Wong, A., Wong, Y. H., Becker, P. C., Bruce, A. J., and Adar, R., "Er³⁺ glass waveguide amplifier at 1.5 μm on silicon." *Electronics Letters*, vol. 28 (13), (1992) p. 1181-1182.
- [8] Guldborg-Kjaer, S., Hubner, J., Kristensen, M., Laurent-Lund, C., Rysholt Poulsen, M., and Sckerl, M. W., "Planar waveguide laser in Er/Al-doped germanosilicate." *Electronics Letters*, vol. 35 (4), (1999) p. 302-303.
- [9] Kitagawa, T., Hattori, K., Shimizu, M., Ohmori, Y. A. Ohmori Y., and Kobayashi, M. A. Kobayashi M., "Guided-wave laser based on erbium-doped

- silica planar lightwave circuit." *Electronics Letters*, vol. 27 (4), (1991) p. 334-335.
- [10] Hoven, G. N. van den, Koper, R. J. I. M., Polman, A., Dam, C. van, Uffelen, J. W. M. van, and Smit, M. K., "Net optical gain at 1.53 μm in Er-doped Al_2O_3 waveguides on silicon." *Appl. Phys. Lett.*, vol. 68 (1996) p. 1886.
- [11] Serna, R., Ballesteros, J. M., Castro, M. Jimenez de, Solis, J., and Afonso, C. N., "Optically active Er-Yb doped glass films prepared by pulsed laser deposition." *Appl. Phys.*, vol. 84 (1998) p. 2352.
- [12] Benatsou, M., Capoen, B., Bouazaoui, M., Tchana, W., and Vilmot, J. P., "Preparation and characterization of sol-gel derived $\text{Er}^{3+}:\text{Al}_2\text{O}_3\text{-SiO}_2$ planar waveguides." *Appl. Phys. Lett.*, vol. 71 (1997) p. 428.
- [13] Huang, W. and Syms, R. R. A., "Sol-gel silica-on-silicon buried-channel EDWAs." *Journal of Lightwave Technology*, vol. 21 (5), (2003) p. 1339-1349.
- [14] Stone, J. and Burrus, C.A., "Nd-doped SiO_2 Lasers in end pumped fibre geometry." *Appl. Phys. Lett.*, vol. 23 (1973) p. 388-389.
- [15] Bebbington, J. A., Barbarossa, G., Bonar, J. R., and Aitchinson, J. S., "Rare-earth doped silica waveguides on Si fabricated by flame hydrolysis deposition." *Applied Physics Letters*, vol. 62 (4), (1993) p. 337-339.
- [16] Bonar, J.R., Bebbington, J.A., Aitchison, J.S., Maxwell, G.D., and Ainslie, B.J., "Low threshold Nd-doped silica planar waveguide laser." *Electronics Letters*, vol. 30 (3), (1994) p. 229-230.
- [17] Hibino, Y., Kitagawa, T., Shimizu, M., Hanawa, F. A. Hanawa F., and Sugita, A. A. Sugita A., "Neodymium-doped silica optical waveguide laser on silicon substrate." *IEEE Photonics Technology Letters*, vol. 1 (11), (1989) p. 349-350.

- [18] Kitagawa, T., Hattori, K., Hibino, Y., and Ohmori, Y. A. Ohmori Y., "Neodymium-doped silica-based planar waveguide lasers." *Journal of Lightwave Technology*, vol. 12 (3), (1994) p. 436-442.
- [19] Townsend, J.E., Poole, S.B., and Payne, D.N., "Solution-doping technique for fabrication of rare-earth-doped optical fibres." *Electronics Letters*, vol. 23 (7), (1987) p. 329-331.
- [20] Kawachi, M., Yasu, M., and Edahiro, T., "Fabrication of SiO₂-TiO₂ glass planar optical waveguides by flame hydrolysis deposition." *Electronics Letters*, vol. 19 (15), (1983) p. 583-584.
- [21] Kawachi, M., "Silica waveguides on silicon and their application to integrated-optic components." *Opt. and Quantum Electron.*, vol. 22 (1990) p. 391-416.
- [22] Barbarossa, G. and Laybourn, P. J. R., "Vertically integrated high-silica channel waveguides on Si." *Electronics Letters*, vol. 28 (5), (1992) p. 437-438.
- [23] Guilhot, Dennis Alain "UV-written devices in rare-earth doped silica-on-silicon grown by FHD," PhD Thesis, Science and Mathematics, Optoelectronics Research Centre, University of Southampton, 2004.
- [24] K.Hattori, Kitagawa, T., Oguma, M., Ohmori, Y., and M.Horiguchi, "Erbium-doped silica based waveguide amplifier integrated with a 980/1530nm WDM coupler." *Electronics Letters*, vol. 30 (11), (1994) p. 856-857.
- [25] Bonar, J. R., Vermelho, M. V. D., McLaughlin, A. J., Marques, P. V. S., Aitchison, J. S., Martins-filho, J. F., Bezerra-Jr, A. G., Gomes, A. S. L., and Araujo, Cid. B. de, "Blue light emission in thulium doped silica-on-silicon waveguides." *Optics Communications*, vol. 141 (1997) p. 137-140.
- [26] Tumminelli, R., Hakimi, F., and Haavisto, J., "Integrated-optic Nd:glass laser fabricated by flame hydrolysis deposition using chelates." *Optics Letters*, vol. 16 (14), (1991) p. 1098-1100.

- [27] Gaydon, A. G. and Wolfhard, H. G., "*Flames*".1970: Chapman and Hall Ltd.
- [28] Sakaguchi, S., "Consolidation of GeO₂ soot body prepared by flame hydrolysis reaction." *Non-crystalline Solids*, vol. 171 (3), (1994) p. 228-235.
- [29] Watts, Samuel Pul, "Flame Hydrolysis Deposition of Photosensitive Silicate Layers Suitable for the Definition of Waveguiding Structures through Direct Ultraviolet Writing," PhD Thesis, Department of Electronics and Computer Science, University of Southampton, 2002.
- [30] Waldron, M. B. and Daniell, B. L., "*Sintering*".1978: Heydon and sons Ltd.
- [31] Scherer, G. W., "Sintering of low-density glasses I: theory." *Am. Ceram. Soc.*, vol. 60 (5-6), (1977) p. 236-239.
- [32] Maxwell, G. D., "Optical waveguide fabrication in silica using flame hydrolysis," PhD, University of Glasgow, 1990.
- [33] Dhar, A., Paul, M. C., Pal, M., Mondal, A. K., Sen, S., Maiti, H. S., and Sen, R., "Characterization of porous core layer for controlling rare earth incorporation in optical fiber." *Opt. Express* vol. 14 (20), (2006) p. 9006-9015.
- [34] Ainslie, B. J., "A review of the fabrication and properties of erbium-doped fibers for optical amplifiers." *Journal of Lightwave Technology*, vol. 9 (2), (1991) p. 220-227.
- [35] Tang, F. Z., McNamara, P., Barton, G. W., and Ringer, S. P., "Multiple solution-doping in optical fibre fabrication I - Aluminium doping." *Journal of Non-Crystalline Solids*, vol. 354 (10-11), (2008) p. 927-937.
- [36] J.E.Townsend, "The development of optical fibres doped with rare earth ions," PhD Thesis, University of Southampton UK, 1990.
- [37] Tang, F. Z., McNamara, P., Barton, G. W., and Ringer, S. P., "Nanoscale characterization of silica soots and aluminium solution doping in optical fibre

- fabrication." *Journal of Non-Crystalline Solids*, vol. 352 (36-37), (2006) p. 3799-3807.
- [38] Gonzalez-Diaz, B., Diaz-Herrera, B., Guerrero-Lemus, R., Mendez-Ramos, J., Rodriguez, V. D., Hernandez-Rodriguez, C., and Martinez-Duart, J. M., "Erbium doped stain etched porous silicon." *Materials Science and Engineering: B*, vol. 146 (1-3), (2008) p. 171-174.
- [39] "*Handbook of Chemistry and Physics*". 58th ed. 1978. Florida: CRC Press.
- [40] Poole, S. B., "Fabrication of Al₂O₃ co-doped optical fibres by a solution-doping technique," in *Optical Communication, 1988. ECOC 88. Fourteenth European Conference on (Conf. Publ. No.292)*, 1988, p. 433-436
- [41] Larsen, C., ed: LYCOM.
- [42] R.Simpson, Jay, "Rare Earth Doped Fiber Fabrication: Techniques and Physical Properties," in *Rare-earth-doped Fiber Lasers and Amplifiers*, Digonnet, Ed., 2 ed New York, USA: Marcel Dekker, Inc, 2001.
- [43] Denker, B. I., Osiko, V. V., Pashinin, P P., and Prokhorov, A. M., "Concentrated neodymium laser glasses (review)." *Soviet J. Quantum Electronics*, vol. 11 (3), (1981) p. 289-297.
- [44] Bondarenko, E. G., Galant, E. I., Lunter, S. G., Przhevskii, A. K., and Tolstoi, M. N., "The effect of water in glass on the quenching of the luminescence of rare-earth activator." *Soviet J. Opticas and Technology*, vol. 42 (1975) p. 333-335.
- [45] Hanawa, F., Sudo, S., Kawachi, M., and Nakahara, M., "Fabrication of completely OH-free v.a.d. fibre." *Electronics Letters*, vol. 16 (18), (1980) p. 699-700.

- [46] Moriyama, T., Fukuda, O., Sanada, K., Inada, K., Edahiro, T., and Chida, K., "Ultimately low OH content v.a.d. optical fibres." *Electronics Letters*, vol. 16 (18), (1980) p. 698-699.
- [47] Hammond, C. R. and Norman, S. R., "Silica based binary glass systems- refractive index behaviour and composition in optical fibres." *Optical and Quantum Electronics*, vol. 9 (1977) p. 399-409.
- [48] Simpson, J. R., "Fabrication of rare-earth doped glass fibers," in *SPIE "Fibre lasers and amplifiers*, Boston, 1989.
- [49] Matejec, V., Sysala, O., Sedlar, M., Kasik, I., and Gotz, J., "Preparation of preforms and fibres containing Na, Mg, Nd, Er, Al, Sb by the MCVD method," presented at the ECOC'89, Gothenberg, 1989.
- [50] Townsend, J. E., "The development of optical fibres doped with rare-earth ions," PhD Thesis, Electronics and Computer Science, University of Southampton, 1990.
- [51] Cotton, D. A. and Wilkinson, G., "*Advanced Inorganic Chemistry*".1972: Wiley Interscience.
- [52] Askins, C., ed.
- [53] Dhar, A., Paul, M. C., Pal, M., Bhadra, S. K., Maiti, H. S., and Sen, R., "An improved method of controlling rare earth incorporation in optical fiber." *Optics Communications*, vol. 277 (2), (2007) p. 329-334.
- [54] Tarbox, E. J., ed.
- [55] Gozen, T., Kikukawa, Y., Yoshida, M., Tanaka, H., and T.Shintani, "Development of high Nd³⁺ content VAD single-mode fiber by molecular stuffing technique," in *Proc. OFC'88*, 1988.

- [56] Saifi, M. A., Andrejco, M. J., Way, W. I., Lehman, A. Von, Yan, A.Y., Lin, C., Bilodeau, F., and Hill, K. O., "Er³⁺-doped GeO₂-CaO-Al₂O₃ silica core fiber amplifier pumper at 813 nm.," in *Proc. OFC'91*, 1991, p. 198.
- [57] Cognolato, L., Sordo, B., Modone, E., Gnazzo, A., and Cocito, G., "Aluminium/erbium active fibre manufactured by a non-aqueous solution doping method.," in *Proc. SPIE*, 1989, p. 202-208.
- [58] Tang, F. Z., McNamara, P., Barton, G. W., and Ringer, S. P., "Multiple solution-doping in optical fibre fabrication II - Rare-earth and aluminium co-doping." *Journal of Non-Crystalline Solids*, vol. 354 (15-16), (2008) p. 1582-1590.

CHAPTER 4

RESULTS AND DISCUSSIONS

4.1 PRE-SINTER TEMPERATURE

As mentioned in the previous chapter, the porosity distribution and pore size of the soot layer is important for solution doping process [1-2]. Soot layer produced by FHD process satisfied the requirement of such porous condition [3]. The FHD layer consists of weakly bonded particles. These bonds are so weak that it can be easily damaged by external force during solution doping. Hence, pre-sinter process was used to increase the bonding strength between the soot particles such that it was partially densified via heat treatment. An optimum pre-sinter temperature would produce a layer with good surface morphology and adhesion to the silicon based substrate. SEM imaging of these pre-sintered samples show a porous layer (refer Figure 4.1). The magnification used is 5000x.

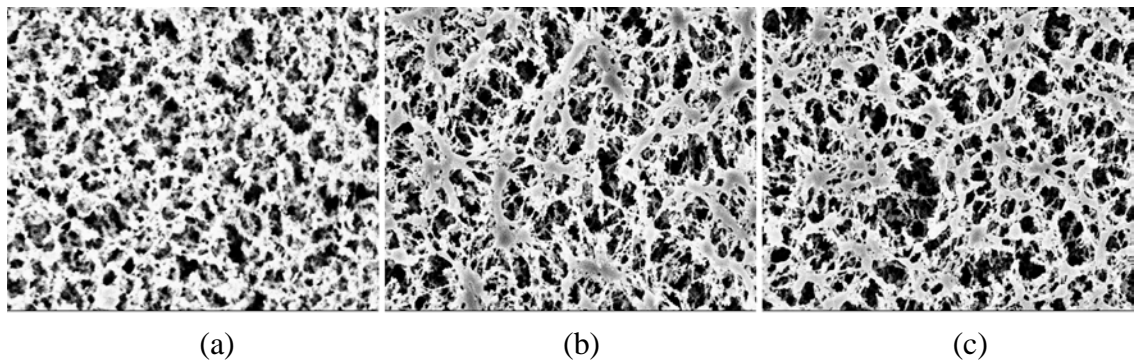


Figure 4.1 SEM images of porous pre-sintered FHD layers at various pre-sintering temperatures; (a) 500°C, (b) 750°C, and (c) 800°C.

Based on the SEM images, no significant differences could be detected in terms of pore size and porosity. All of these pre-sintered samples were found highly aqueous-absorbing. However, layers that were pre-sintered below 750°C would be diluted upon immersion in solution. The layer integrity could not be retained well which eventually

leads to disengagement of soot layer from the substrate. On the other hand, those pre-sintered around 750C adhered to the silicon substrate upon immersion but develop cracks when subjected to drying. This phenomenon is most probably related to the differences of thermal expansion characteristic for the soot layer and the silicon substrate.

During the dehydration of rare-earth doped soot in oven, liquid evaporation contraction might cause shrinkage within the soot layer while silicon substrate encountered expansion. Hence, there would be a great possibility that cracks will occur in the soot layer as the bonding between the soot particles is not strong enough. This issue was easily solved by increasing the pre-sinter temperature. Layers pre-sintered above 800°C showed the best results in terms of surface integrity and absence of cracking. This was indicated as in figure 4.2(c)

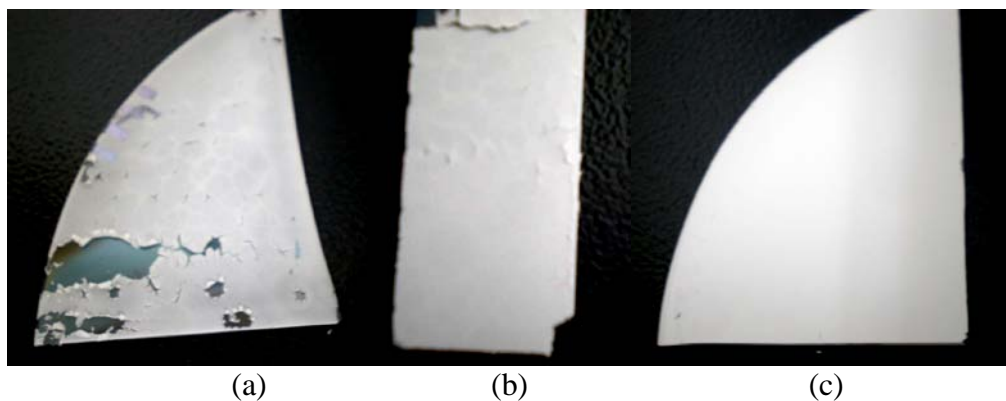


Figure 4.2 Defects induced by solution doping (a) 500°C (b) 750°C (c) 800°C

4.2 FULLY-SINTERED AND HALF-SINTERED DOPED SILICA FILMS

In most of the previously reported work on solution doping, the dopants concentration in the porous half sintered soot layer was not showed. The changes of the dopants concentration in the partially sintered soot layer to fully dense glass layer were not well known. Few set of samples have been solution doped and characterization was done on both the half-sintered (at $\sim 850^\circ\text{C}$) and fully sintered (at $\sim 1350^\circ\text{C}$) silica layer.

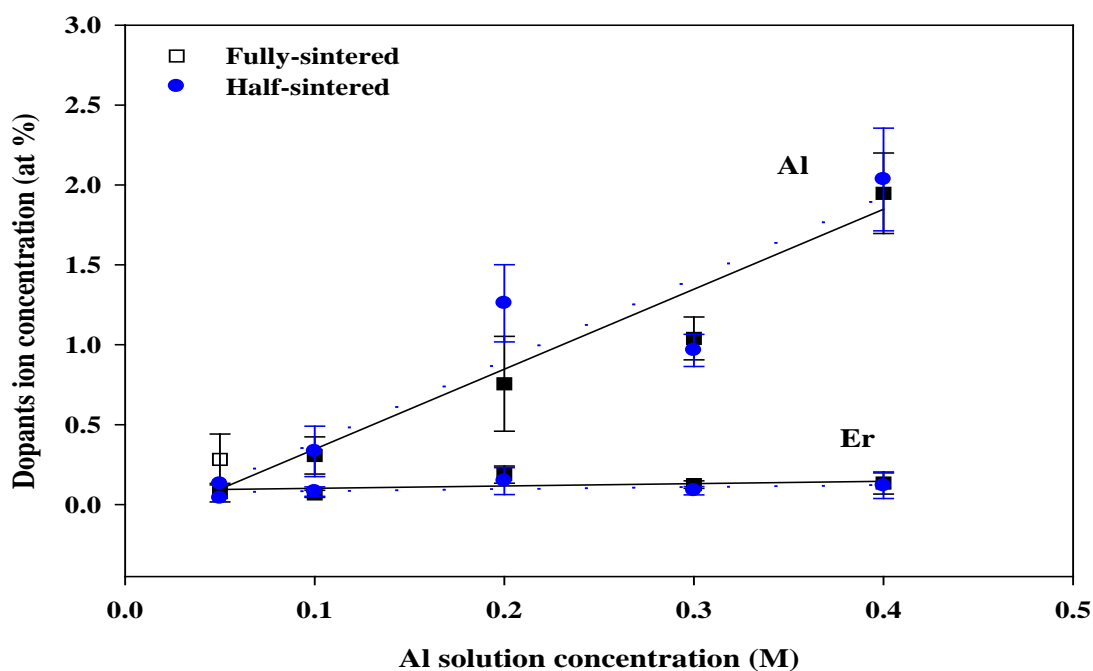


Figure 4.3 Variation of Al and Er concentration in planar film with change in Al solution concentration for a fixed 0.02M Er solution.

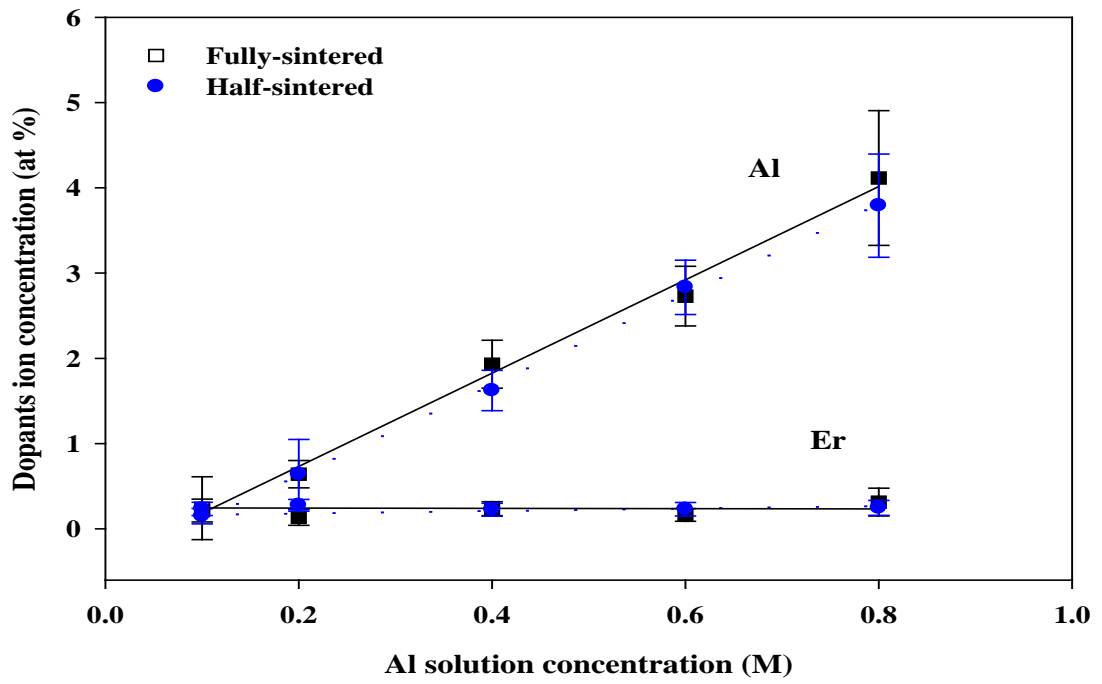


Figure 4.4 Variation of Al and Er concentration in planar film with change in Al solution concentration for a fixed 0.04M Er solution.

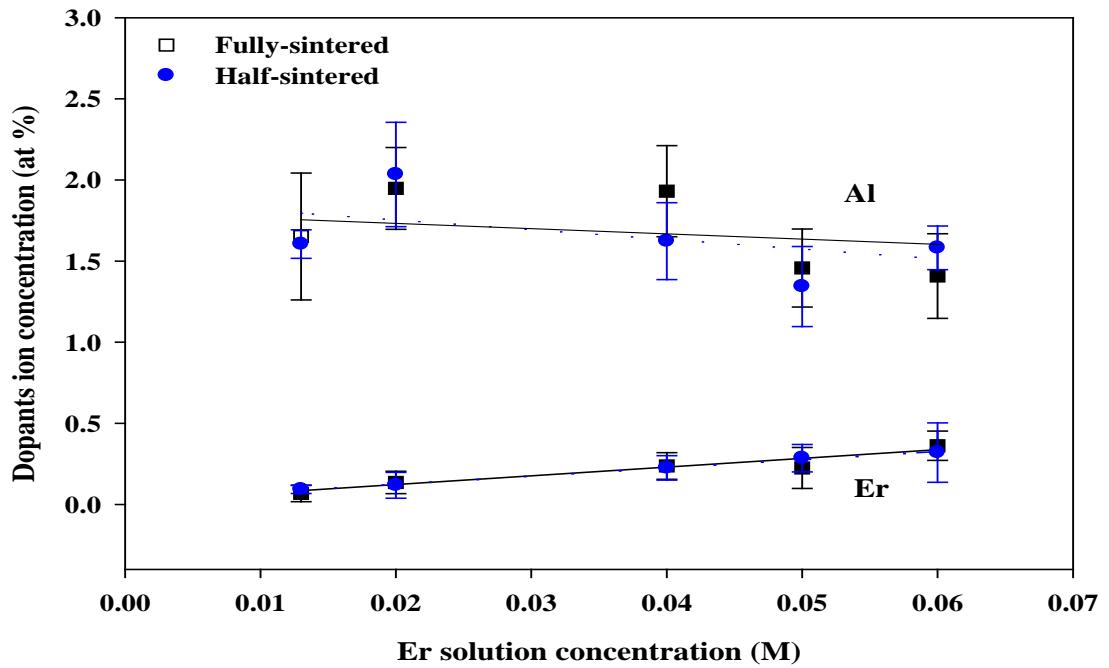


Figure 4.5 Variation of Al and Er concentration in planar film with change in Er solution concentration for a fixed 0.4M Al solution.

The dopants concentration observed in both full-sintered glass film and half-sintered soot layer was illustrated as in Figures 4.3-4.5. Both Figure 4.3 and 4.4 show the variation of dopants concentration as a function Al solution concentration but with two individual Er solution strength (0.02M and 0.04M). The Al concentration shows a linear increment as the Al solution concentration increases.

Er concentration did not show significant changes since its absolute value was relatively small compared to Al. In fact, the Er concentration contained a slight increment as Al solution strength become stronger. This will be further elaborated in section 4.4 (refer figure 4.8).

As indicated in the figure, the trend of the line for full-sintered glass film was found analogous to the half-sintered soot layer. The dopants concentration did not seem to be affected much by the high heating process for full sintering to form a glass film.

In addition, the proportionality between the Er concentration and Er solution concentration increased with the Al solution concentration fixed at 0.4M. Meanwhile, the Al concentration encountered a slight decrement as the Er solution strength increases. Overall, both the full-sintered glass film and half-sintered soot layer shared the same trend.

4.3 EFFECT OF ERBIUM CONCENTRATION

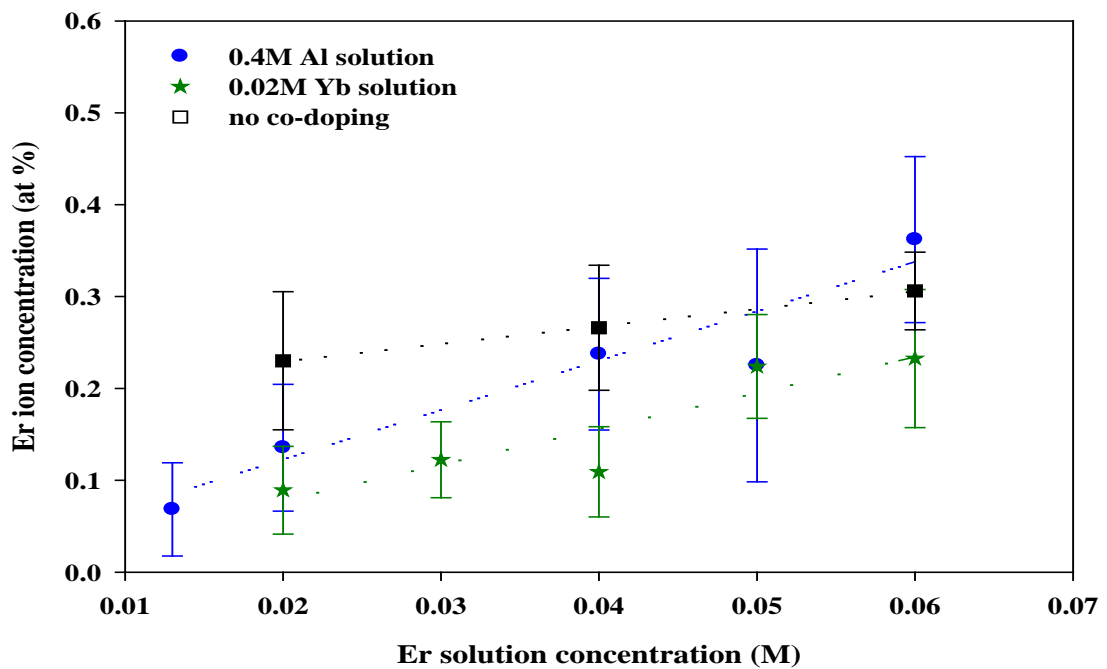


Figure 4.6 The variation of Er concentration in the silica films as a function of Er solution concentration.

Figure 4.6 show the variation of Er concentration as a function of the Er solution concentration used during the solution doping process. The results show that the Er concentration in the fully sintered silica films increased linearly with the concentration of Er in solution. Hence, it has been shown that the concentration of Er doped into the sintered film could be controlled by changing the concentration of Er solution. The maximum concentration of Er doped into the glass film was measured to be 0.306 at% for 0.06M Er solution.

The variation of Er concentration for Yb and Al as co-dopant behaved the same as well. From Figure 4.6, we noticed that the gradient of both lines with co-dopants is larger compared to the line without co-dopant. This means that the existence of Al and Yb as co-dopant tend to increase the solubility of Er in silica matrix. The effect of Al as a network modifier (mentioned in Chapter 2) in this case is more significant compare to the Yb. The Er concentration after co-doping was lower than the single Er doped. This

does not reveal the actual doping concentration in the co-doped film. The absolute quantity of Er was actually reduced due to the additional elements such as Al and Yb.

4.4 EFFECTS OF ALUMINIUM IN ERBIUM DOPED SILICA FILMS

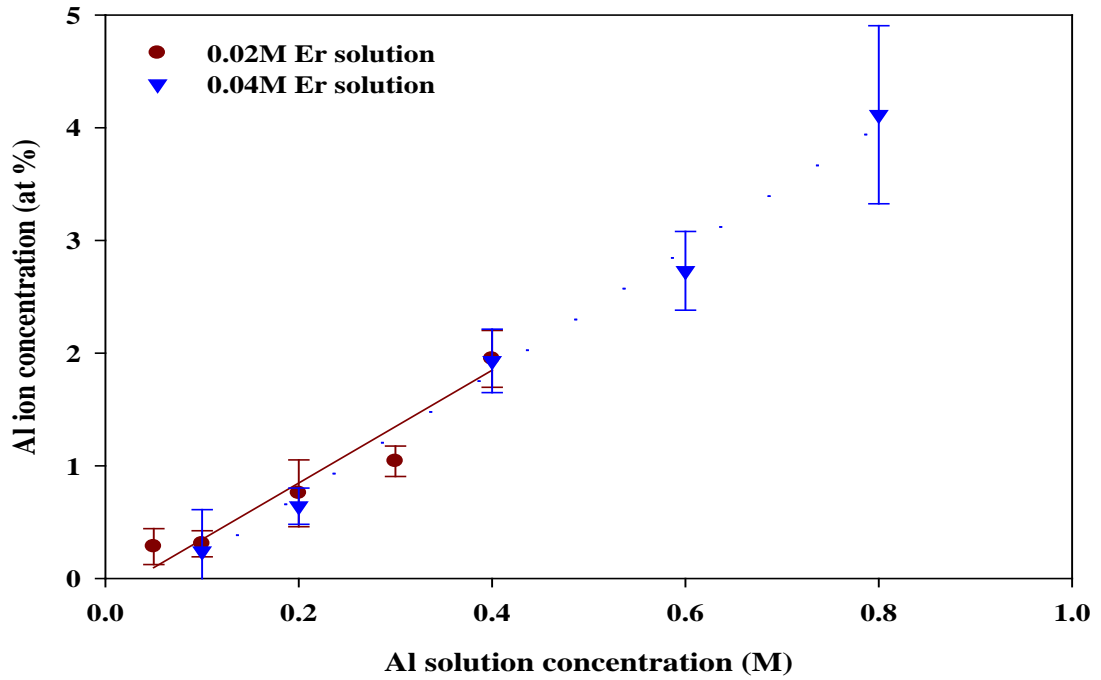


Figure 4.7 The variation of Al concentration in silica film as a function of Al solution concentration.

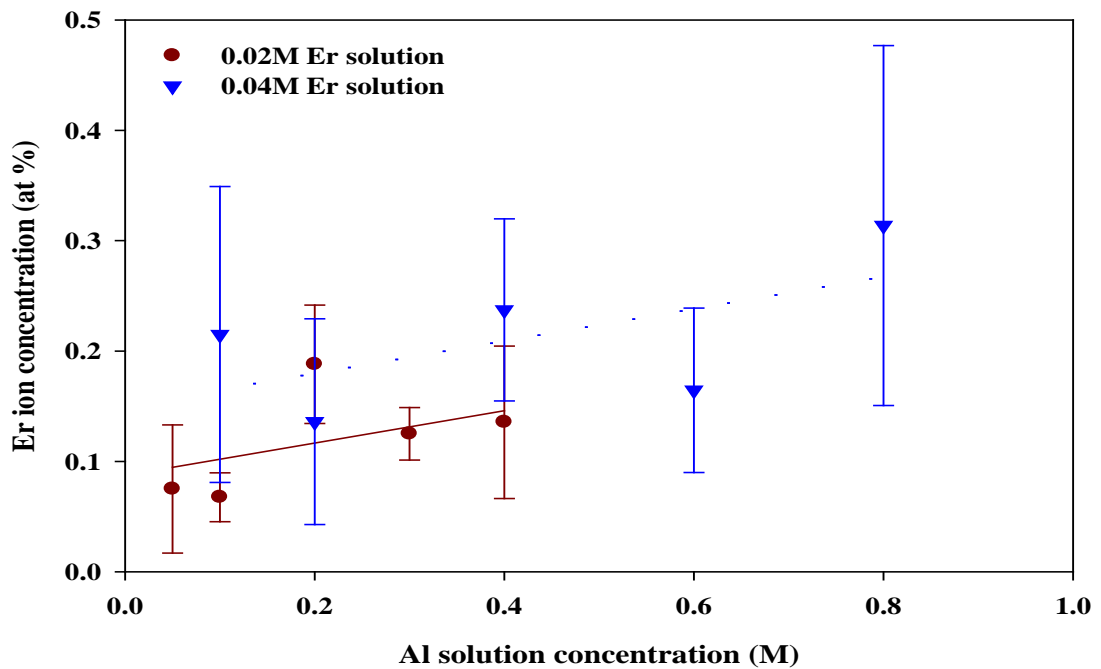


Figure 4.8 The variation of Er concentration in silica film as a function of Al solution concentration.

Figure 4.7 and Figure 4.8 show the variation of dopants concentration as a function of Al solution concentration. Two different Er solution concentrations (fixed at 0.02M and 0.04M) were used. As expected, the Al concentration in the sintered silica film increased linearly with the Al solution concentration. Similar behaviour occurred to the Er concentration doped in the glass film. The variation in Al solution concentration corresponding to a fixed 0.02M (or 0.04M) Er solution concentration leads to changes in the amount of Er doped in silica film. Er concentration doped in the silica film was slightly increased as the Al solution concentration increases [4]. This proved that the addition of Al has facilitated the impregnation of Er into soot layer [5]. It has been proposed that Al^{3+} ions tend to form a 'solvation shell' around the rare-earth and prepare the rare-earth ion for incorporation in silica network [6].

Higher Er concentration (~0.31 at%) can be achieved by co-doping with 0.8M Al, but this usually result in devitrification [7]. Figure 4.8 also exhibit that the Er concentration in the silica film increased as the Er solution used varied from 0.02M to 0.04M. Again, Er concentration was dependent on the solution strength.

4.5 EFFECTS OF YTTERBIUM IN ERBIUM DOPED SILICA FILMS

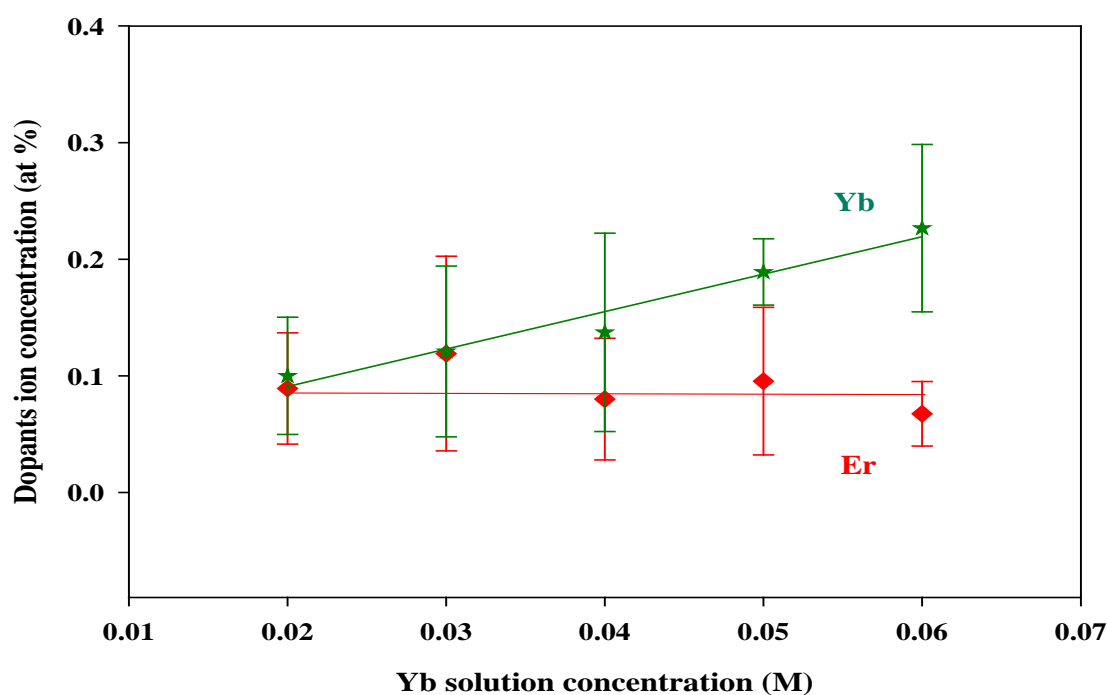


Figure 4.9 Variation of Er and Yb ions concentration in silica film as a function of Yb solution concentration (Er solution concentration fixed at 0.02M).

Study on the effect of solution doping in different Yb solution concentration with an Er solution concentration fixed at 0.02M has been carried out. The variation of Er and Yb concentration in silica films as a function of Yb solution concentration is illustrated in Figure 4.9. As expected, the Yb concentration increased as the Yb solution concentration increases. Er concentrations were remained almost constant at ~0.1 at% which was unaffected by the increasing concentration of Yb solution.

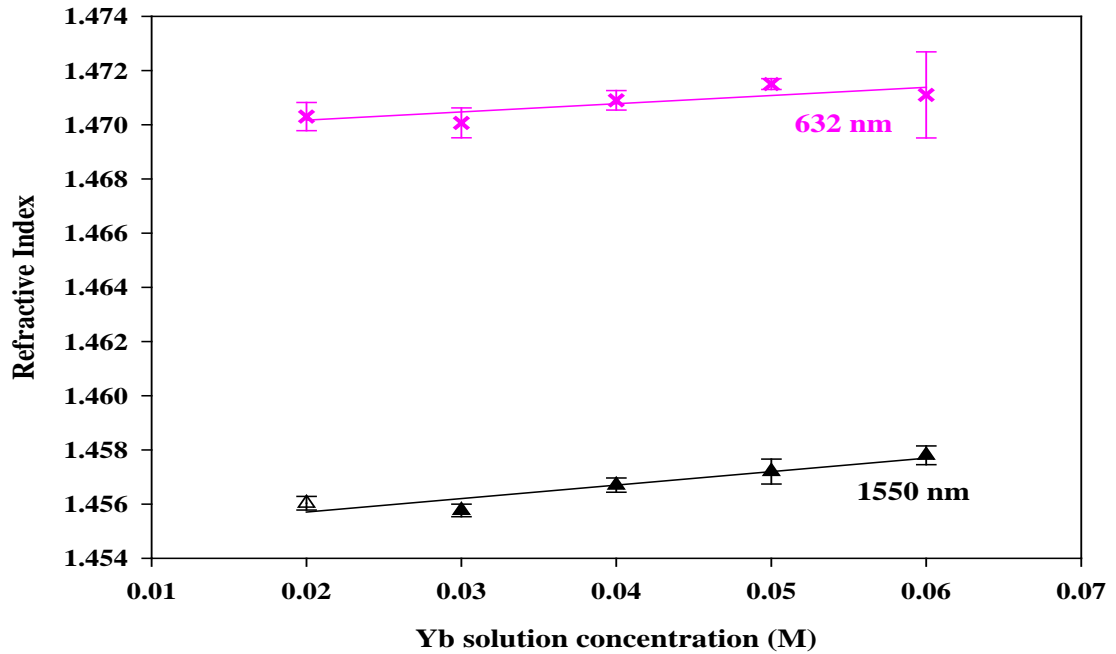


Figure 4.10 Refractive index of Er/Yb doped silica films as a function of Yb solution concentration.

There are reports that the addition of ions with a large radius such as Er and Yb tend to increase the dipole strength of the non-bridging oxygen and hence increase the refractive index [8-10]. Figure 4.10 shows the variation of refractive index corresponding to the Yb solution concentration for a fixed solution concentration of Er at 0.02M. The results indicated that the refractive index observed from both 632nm and 1550nm wavelengths were increased linearly as the Yb solution concentration increases. This behaviour was completely compatible to the Yb concentration shown in the Figure 4.9 which was increased linearly as well.

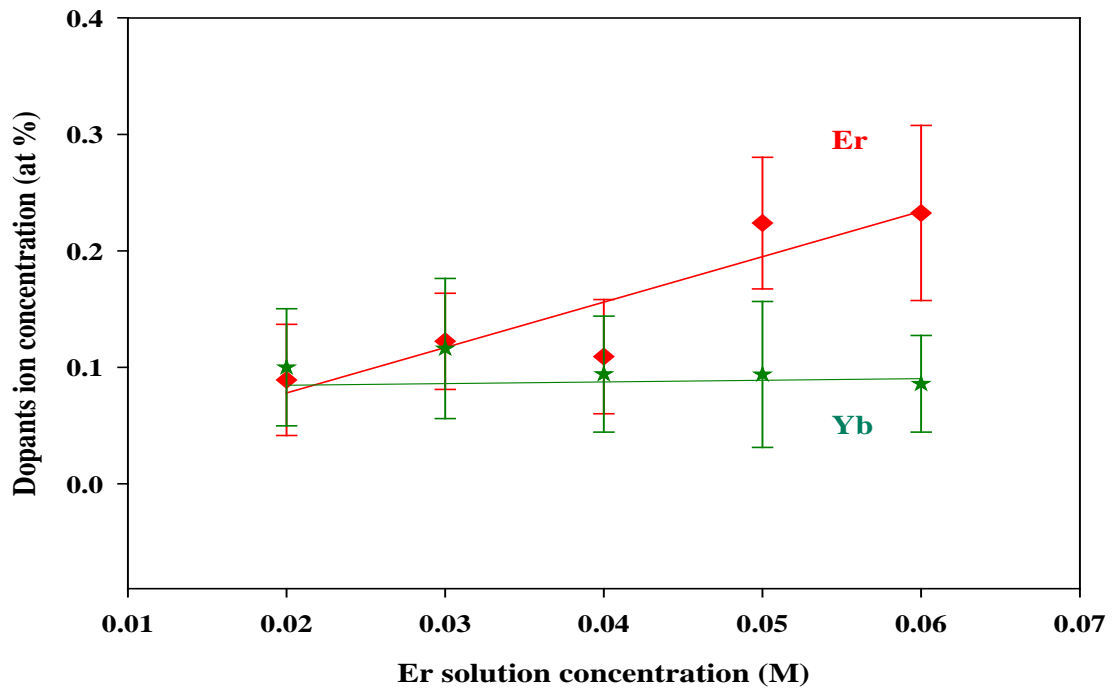


Figure 4.11 Variation of Er and Yb ions concentration in silica film as a function of Er solution concentration (Yb solution concentration fixed at 0.02M).

The incorporation of Er ion in the silica film depending on solution concentration for a fixed 0.02M Yb solution concentration is shown in Figure 4.11. Er concentration was found to increase linearly when the Er solution concentration was increased from 0.02M to 0.06M. As the Yb solution was kept at the concentration of 0.02M, the Yb ion concentration was observed to be remained almost constant.

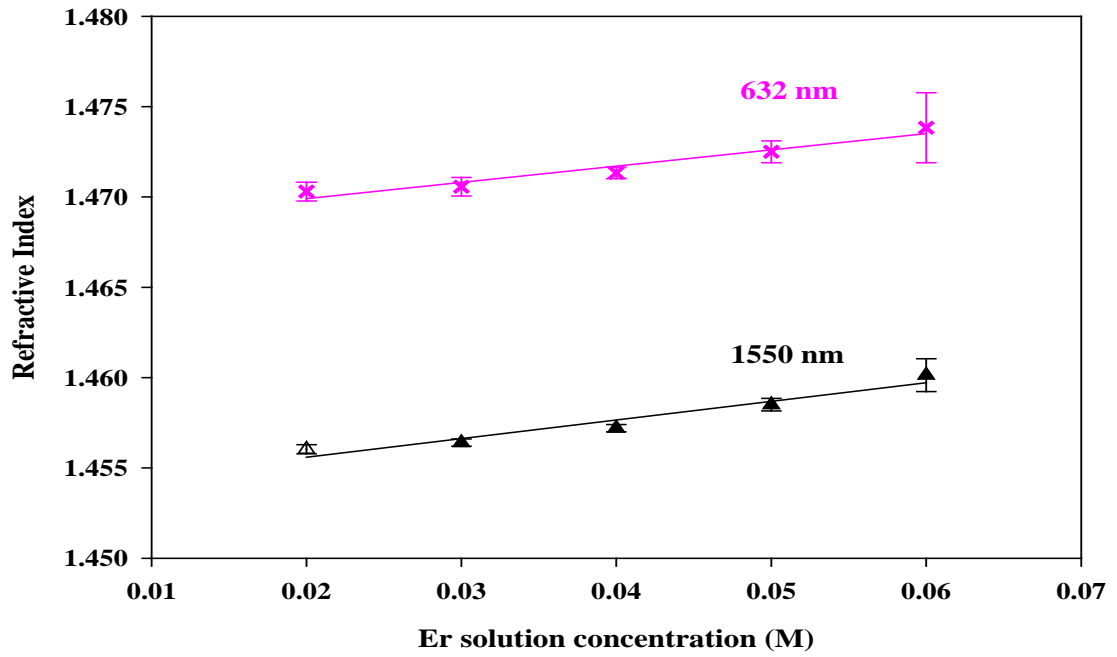


Figure 4.12 Refractive index of Er/Yb doped silica films as a function of Er solution concentration.

Since the Er concentration in the silica film was increased, the trend of its refractive index was expected to be similar. Two wavelengths were used to obtain the refractive index of the related Er/Yb doped silica glass layer. The results indicate that the refractive index increased linearly as the Er solution concentration increases.

4.6 ALUMINIUM AND YTTERBIUM IN CO-DOPING

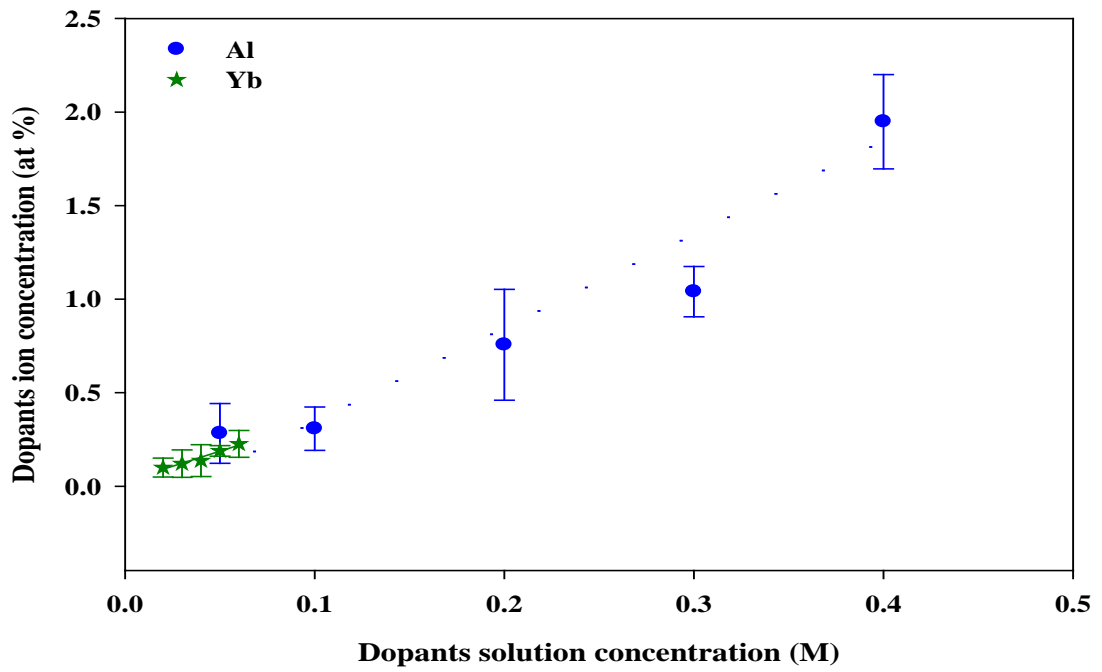


Figure 4.13 The variation of Al and Yb dopants concentration as a function of Al and Yb co-dopants solution concentration.

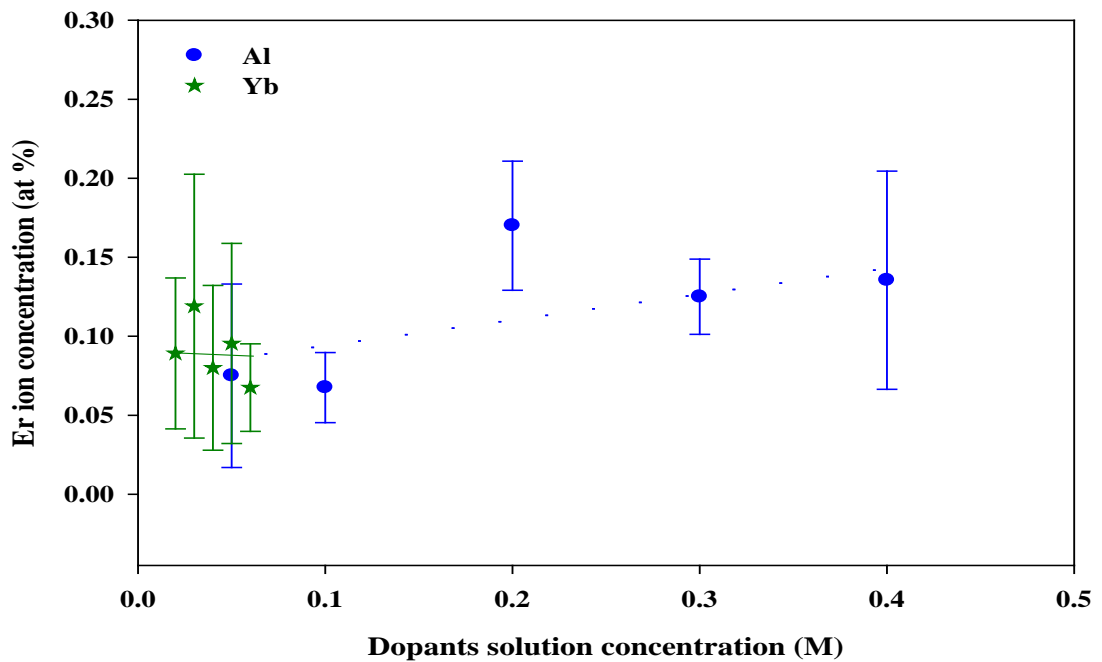


Figure 4.14 The variation of Er concentration in silica film as a function of Al and Yb co-dopants solution concentration.

The Al concentration in silica film increased as Al solution concentration increases. This behaviour was observed the same for the Yb doped silica film; Yb concentration in silica film increased linearly as the concentration of Yb solution increases. In this section, the effect of these two co-dopants on the Er concentration in silica film was investigated. In order to simplify this investigation, a 0.02M Er solution was used. Co-dopants were added in individually in two different solutions for solution doping. The Er/Al doped silica films obtained consist of an elevated Er concentration. This explained that the Al did facilitate in altering the silica matrix to enhance the solubility of Er. Meanwhile, the Er concentration did not change much in terms of solubility when higher Yb solution concentrations were being used.

4.7 IMMERSION PERIOD

The typical immersion period used in solution doping was maintained around 60-90 minutes. Though, there was no significant explanation to such selection but it was considered to be sufficient for a complete solution doping. The optimum immersion period is simply dependent on a few criteria: soot layer thickness, porosity, composition, solvent characteristic and solution strength [4].

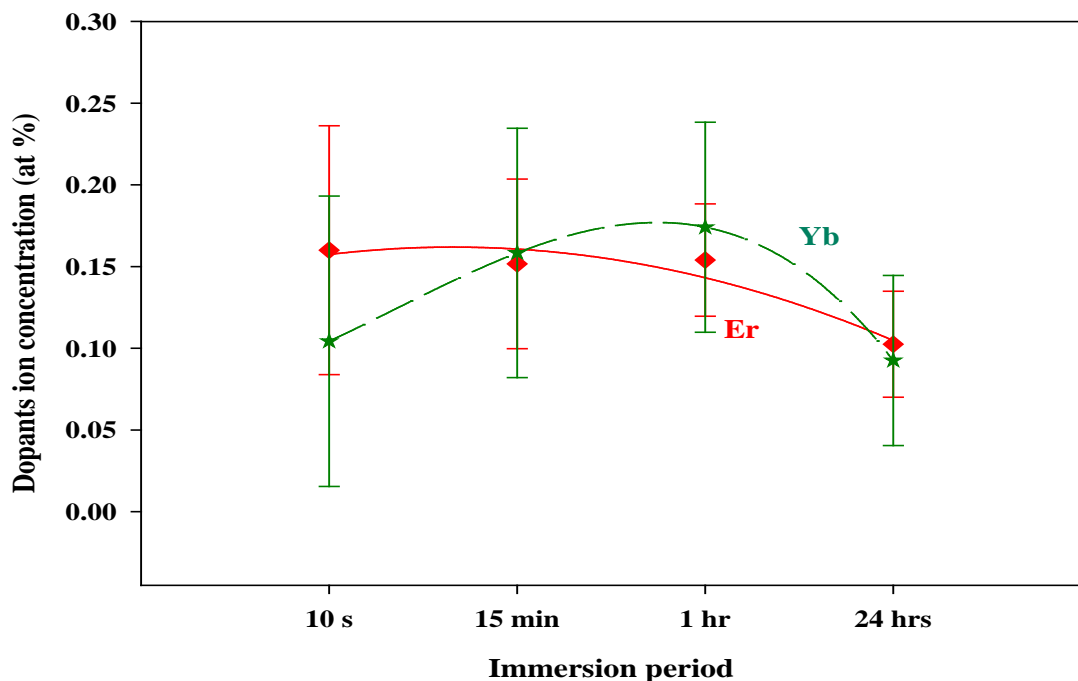


Figure 4.15 The variation of Er and Yb ions concentration as a function of immersion period.

Few identical samples were solution doped in a 0.02M Er/Yb (with ratio 1) solution for four different doping period. The results indicated that the Yb concentration increased as much as 60% when immersion period was elongated from 10 seconds to 15 minutes. As the immersion period increased to 1 hour, the increment rate has become flatter where Yb concentration was raised up to 9.4%. The Yb concentration was then fall to 0.09 at% at 24 hours which is 47% lower than the concentration observed for 1 hour. Meanwhile, not much change in Er concentration doped for the first three doping period but the concentration drops to a minimum value at 24 hours doping period. One

interpretation of this phenomenon is that dopants concentration tends to deteriorate if the doping period was dragged too long. However, the reason for this behaviour is still unknown and will be investigated in future.

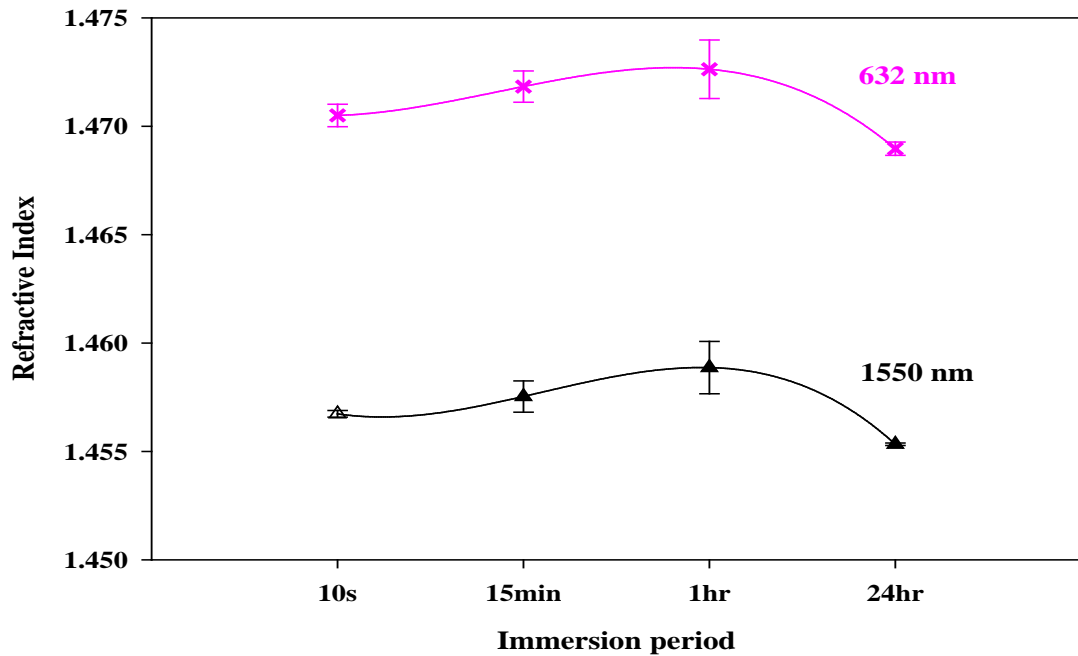


Figure 4.16 Variation of refractive index of Er/Yb doped silica films as a function of immersion period.

The refractive index was significantly influenced by the dopants concentration in the silica films [11]. From Figure 4.16, it was observed that the refractive index increased gradually from doping period of 10 second to 15 minutes and reached a maximum value at 1 hour. However, the refractive index obtained at 24 hours immersion period was found to reach the lowest value. The trend was similar as the Figure 4.15.

4.8 MULTIPLE SOLUTION DOPING

The discussion earlier shows that wide variation in the dopants concentration could be achieved by altering either the solution strength or immersion period. In this section, a new method of solution doping was implemented – multiple soaking of a porous soot layer with intermediate heat-treatment stages (at ~800 °C) between soakings. As mentioned in Chapter 3, this stage is critical as it converts the soluble hydrated chloride salts into insoluble oxides and hence prevents dissolution during multiple soaking. Therefore, enable the retention of dopants in silica layers. Figure 4.17 shows the variation of Er/Yb ion concentration as a function of number of doping cycles.

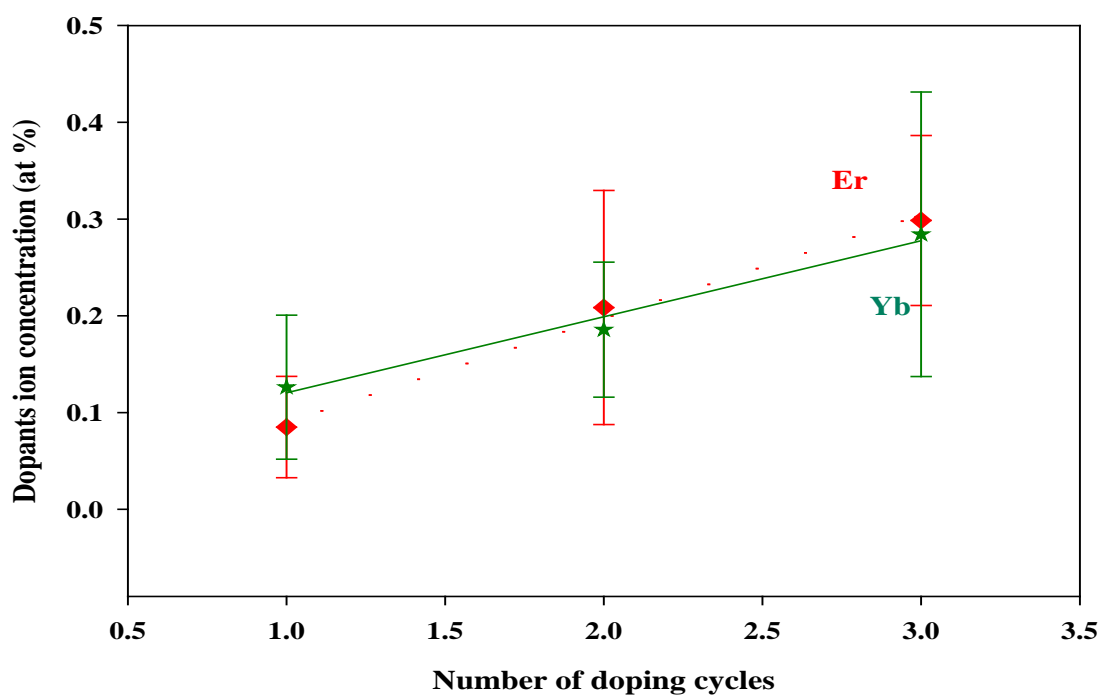
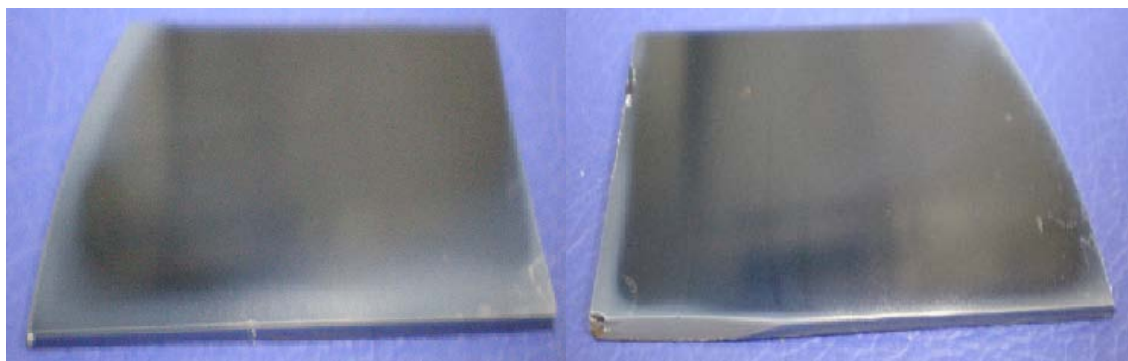


Figure 4.17 Er and Yb ions incorporation in silica film as a function of the number of doping cycles.

The concentration of solution used during multiple solution doping was a mixture of 0.02M Er and 0.02M Yb. Both of the Yb and Er concentration doped in the silica films were increased linearly as the number of doping cycle increased. The Er concentration observed from single doping was 0.085 at % and eventually increased to 0.21 at% when solution doped twice. This increment can still be observed in the three

cycles of solution doping, which is 251.26 % higher than the single doping. Similar behaviour occurred for the Yb concentration. For the single doping, 0.13 at% of Yb was successfully doped in the silica film followed by 0.18 at% for doping twice and finally 0.28 at% for three doping cycles.

The results indicated that it is possible to approach a higher dopant concentration in silica films by multiple solution doping. This method can be applied by using just one solution concentration without the need of varying the concentration of dopant solution. Multiple solution doping has been demonstrated by Tang et al. for single doping and two elements doping [12-13]. It was noted that the silica film in the single doping cycle was transparent while the silica film in two and three doping cycle case were partially opalescent (refer Figure 4.18).



(a) (b)
Figure 4.18 Silica wafer indicating opalescence due to multiple solution doping (a) two doping cycles (b) three doping cycles.

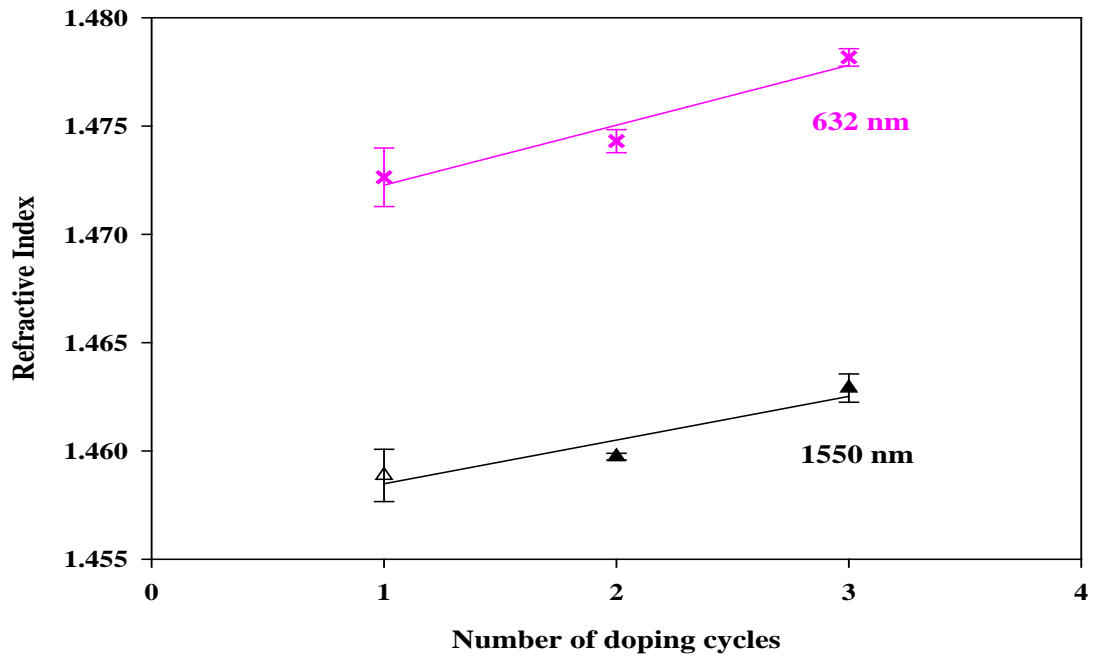


Figure 4.19 Variation of refractive index of Er/Yb doped silica films as a function of number of doping cycle.

Figure 4.19 shows the changes of refractive index as a function of number of doping cycles using 632nm and 1550nm wavelength. The refractive index at both wavelength of 632nm and 1550nm increased linearly as the doping cycle increases. This has confirmed the result from the previous discussion indicating that the dopants concentration increased as the number of doping cycles increase.

REFERENCES:

- [1] Tang, F. Z., McNamara, P., Barton, G. W., and Ringer, S. P., "Nanoscale characterization of silica soots and aluminium solution doping in optical fibre fabrication." *Journal of Non-Crystalline Solids*, vol. 352 (36-37), (2006) p. 3799-3807.
- [2] Dhar, A., Paul, M. C., Pal, M., Mondal, A. K., Sen, S., Maiti, H. S., and Sen, R., "Characterization of porous core layer for controlling rare earth incorporation in optical fiber." *Opt. Express* vol. 14 (20), (2006) p. 9006-9015.
- [3] Guilhot, Dennis Alain "UV-written devices in rare-earth doped silica-on-silicon grown by FHD," PhD Thesis, Science and Mathematics, Optoelectronics Research Centre, University of Southampton, 2004.
- [4] Dhar, A., Paul, M. C., Pal, M., Bhadra, S. K., Maiti, H. S., and Sen, R., "An improved method of controlling rare earth incorporation in optical fiber." *Optics Communications*, vol. 277 (2), (2007) p. 329-334.
- [5] Dhar, A., Pal, A., Paul, M. C., Ray, P., Maiti, H. S., and Sen, R., "The mechanism of rare earth incorporation in solution doping process." *Opt. Express* vol. 16 (2008) p. 12835-12846
- [6] Arai, K., Namikawa, H., Kumata, K., Honda, T., Ishii, Y., and Handa, T., "Aluminium or phosphorus co-doping effects on the fluorescence and structural properties of neodymium-doped silica glass." *Appl. Phys.*, vol. 59 (1986) p. 3430-3436.
- [7] Townsend, J.E., Poole, S.B., and Payne, D.N., "Solution-doping technique for fabrication of rare-earth-doped optical fibres." *Electronics Letters*, vol. 23 (7), (1987) p. 329-331.

- [8] Ro, Sung Ing, Jung, TYong Soon, and Shin, Dong Wook, "The effects of Er/Al co-doping on the fluorescence of silica waveguide film." *Journal of Ceramic Processing Research*, vol. 2 (4), (2001) p. 155-159.
- [9] Barbarossa, G. and Elettronico, I., "Planar silica optical device technology." *Giovanni Barbarossa MCMXCII*, (1992) p. 152-157.
- [10] Lee, Jeong Woo and Chung, Hyung Kon, "Fabrication of borophosphosilicate glass thin films for optical waveguides using Aerosol Flame Deposition method." *J. of Korean Ceramic Society*, vol. 37 (2), (2000) p. 117-121.
- [11] Vienne, G. G., Caplen, J. E., Liang, Dong, Minelly, J. D. A. Minelly J. D., Nilsson, J. A. Nilsson J., and Payne, D. N. A. Payne D. N., "Fabrication and characterization of $\text{Yb}^{3+}:\text{Er}^{3+}$ phosphosilicate fibers for lasers." *Journal of Lightwave Technology*, vol. 16 (11), (1998) p. 1990-2001.
- [12] Tang, F. Z., McNamara, P., Barton, G. W., and Ringer, S. P., "Multiple solution-doping in optical fibre fabrication I - Aluminium doping." *Journal of Non-Crystalline Solids*, vol. 354 (10-11), (2008) p. 927-937.
- [13] Tang, F. Z., McNamara, P., Barton, G. W., and Ringer, S. P., "Multiple solution-doping in optical fibre fabrication II - Rare-earth and aluminium co-doping." *Journal of Non-Crystalline Solids*, vol. 354 (15-16), (2008) p. 1582-1590.

CHAPTER 5

CONCLUSION AND FUTURE WORK

5.1 CONCLUSION

In this research, the solution doping method was successfully applied to form Er/Al and Er/Yb co-doped silica waveguide films deposited by FHD. The morphology inspection indicated that the integrity of the deposited porous soot layer depends heavily on the pre-sinter temperature. The ultimate choice of the pre-sinter temperature must at least provide a good soot adherence to substrate and free from crack upon solution doping. Based on the results, the soot layer pre-sintered at around 800°C fulfills the required quality.

The investigation also revealed that the dopants concentration in silica films was dependent on a few dipping parameters which includes the solution strength and immersion period. The influence of the solution strength was more significant since the concentration observed exhibited a linear relationship with the solution concentration. However, increasing the solution concentration for achieving a desired doping concentration is not a viable option. This is because by increasing the solution concentration, the solution becomes more viscous and this might cause a reduction in the extension of the solution during penetration into soot film. The increment in the refractive index of the doped silica films was believed to have been caused by the existence of the rare-earth ions. The higher the rare-earth concentration, the higher the refractive index would be.

Meanwhile, the interdependence of immersion period with dopants concentration was obvious as the impregnation of dopants became higher when the doping period increases. However, the concentration deteriorated when the solution doping process was elongated till 24 hours. Therefore, proper selection of immersion period can be adjusted to ensure the completeness of solution doping process.

The effect of two different co-dopants in Er concentration was elaborated in Sections 4.3 and 4.6. The use of Al was prove to increase the solubility of Er in silica matrix and hence increased the Er concentration obtained in silica film. The proportionality between the Er concentration in silica films and Al solution concentration increased without the need of increasing the Er solution strength. On the other hand, the solubility of Er increased with the addition of Yb as well although not as significant as in the Al case. Even so, the concentration of Er was not affected much when the solution concentration of Yb was increased.

The effect of sintering temperature on the dopants concentration was briefly examined by comparing the dopants concentration obtained from both the partially porous doped silica films and fully densified doped silica films. Both types of samples shared a similar concentration reading with no significant changes in terms of dopants concentration. Therefore, it was assumed that the dopants concentration observed in the sintered film (sintered at $\sim 1350^{\circ}\text{C}$) actually identified the dopants concentration in the porous film.

New method of solution doping was applied in preparing the Er/Yb silica film – multiple solution doping. This method was used to study the influence of soaking cycle to the dopants concentration in silica film using a low solution concentration with a fixed immersion period. It is a technique that was modified from the original work by F.Z. Tang and colleges. Heat-treatment at 800°C must be used between solution

soaking as it was crucial to convert the soluble hydrated chloride salts in porous film into insoluble oxide for dopants retention. The results indicated that the multiple solution doping can be used to increase the amount of Er/Yb to be incorporated in silica films.

5.2 FUTURE WORK

In general, short path length of planar optical amplifiers required a higher doping concentration as the basic need to observe higher gain. Therefore, high solution concentration was used in this experiment. However, the edge part of the sample was observed to be partially opalescent compared to the transparent middle part at high concentration doping. It was believed to have been caused by devitrification due to high concentration doping. However, there is no significant proof for such phenomenon. In this case, X-ray Diffraction is suggested to be used for verifying crystallization.

For a typical EDX technique, the X-rays are generated in a region about 2 microns in depth. Thus, the concentration profile beyond 2 microns in the silica film was not known. Auger Electron Spectroscopy (AES) is capable of probing the first few monolayers of a surface. This can be applied to study the depth profile of the doped silica layer when used with Refractive Ion Etching (RIE). Hence, it allows us to reveal the concentration gradient occurring within the silica layer.

The solution doping method was successfully applied to form Er/Al and Er/Yb co-doped silica waveguide films deposited by FHD. Hence, this solution doping technique can be used to fabricate a complete optical amplifier. The FHD layer shall include three layers: with undercladding, core and overcladding. Optical test such as spontaneous emission and gain measurements can be implemented.